WL-TM-91-311-FIBG

NONLINEAR ASPECTS OF AEROSPACE STRUCTURES AT HIGH EXCITATION LEVELS FLAT ALUMINIUM BEAMS AND PLATES STUDIED
PROGRESS REPORT OCT 89 - SEP 90

Howard F. Wolfe

Acoustics and Sonic Fatigue Group
Structural Dynamics Branch

MAY 1991

Approved for public release; distribution is unlimited.

FLIGHT DYNAMICS DIRECTORATE
WRIGHT LABORATORY
WRIGHT-PATTERSON AIR FORCE BASE, OH 45433

DISCLAIMER NOTICE

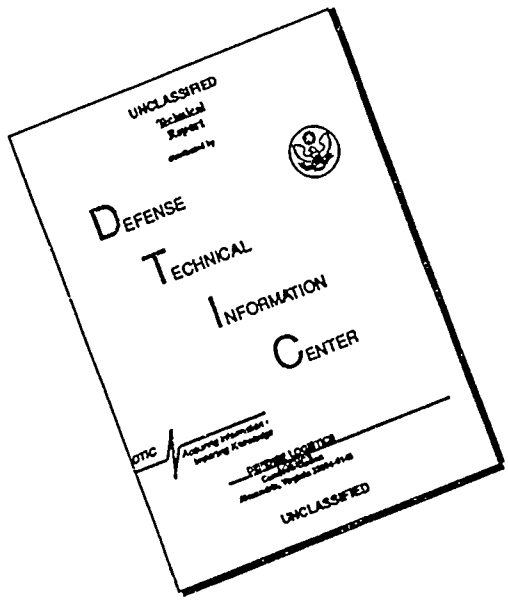

THIS DOCUMENT IS BEST QUALITY AVAILABLE. THE COPY FURNISHED TO DTIC CONTAINED A SIGNIFICANT NUMBER OF PAGES WHICH DO NOT REPRODUCE LEGIBLY.

FORWORD

This memorandum documents essentially the information contained in a MPhil/PhD Progress Report submitted August 1990 to Professor R.G. White at the Institute of Sound and Vibration Research (ISVR), University of Southampton, England. The work was performed under the supervision of Professor R.G. White as part of a long term full time training (LTTFT) program Oct 1989 to Sep 1990. The thesis topic and description were approved as part of the LTTFT by Jerome Pearson, Chief, Structural Dynamics Branch, WL/FIBG, Wright-Patterson AFB, Ohio.

Prepared by:

Howard F. Wolfe

Howard F. Wolfe, Aerospace Engineer
Acoustics & Sonic Fatigue Group

Ralph M. Shimovetz, Tech Manager
Acoustics & Sonic Fatigue Group

This report has been reviewed and approved.

Jerome Pearson

Jerome Pearson, Chief
Structural Dynamics Branch
Structures Division

Accession For	
NTIS GRA&I	☑
DTIC TAB	☐
Unannounced	☐
Justification	
By	
Distribution/	
Availability Codes	
Dist	Avail and/or Special
A-1	

ABSTRACT

Nonlinear multimodal response of flat aluminium clamped beams and plates was studied theoretically and experimentally together with associated signal processing effects. The study does not include buckling effects, curved structure, or sandwich structures. A review of the applicable literature and current research work was made. Theoretical models were evaluated to determine the various methods investigated and which methods might yield new information if further development with specific applications were pursued. The test methods and transducer suitability were carefully scrutinized. Beam tests were performed with sinusoidal and random excitation using a coil-magnet exciter. Clamped flat plate tests were performed using high intensity acoustic excitation from low levels to high levels. Data processing and analysis were investigated to determine their suitability. The hard spring nonlinearity or jump phenomena was apparent from the beam test results. The beam and plate were instrumented to separate the bending and axial components from the total strain. Displacement shapes of the beam were completed. The beam tests and the acoustic tests with the plate have been completed. Peak broading effects and multimodal response were observed.

CONTENTS

1.0 INTRODUCTION

Many factors over past years have led to increased acoustic loads on aerospace structures while future structural configurations with new materials and much higher stiffness-to-weight ratios are evolving. One aspect of the problem is the response of structures due to increasing loads while the configurations and materials of interest are stiffer and more lightweight.

Extensive work has been produced in acoustic fatigue and related technologies. Curved and sandwich types of structures will not be included in this work. Buckling and high temperature behaviour of structures are not included. Also the fatigue behaviour including characterisation for anisotropic materials is not included. The focus of the work was the understanding of the nonlinear structural response at high loading rates and the phenomena involved. Multi-modal behaviour of simple flat beams and plates to sinusoidal and random excitation up to five times the thickness of the structures was considered. Homogeneous lightweight materials applicable to aerospace structures, such as aluminium, was considered first. The statistical properties of strain or stress response behaviour and the loading was addressed.

2.0 THEORETICAL CONSIDERATIONS

Various design guides were compiled (1,2) for predicting the acoustic fatigue life of mostly metallic structures using semi-empirical mathematic expressions and design nomographs. The predictions were based upon assuming the fundamental mode as the controlling parameter which simplified the analysis. Miner's law of cumulative damage theory and a range of experimental results from various structures were utilized. Design guides were continued by ESDU International plc (Engineering Science Data Unit) in London UK and updated periodically for use in the government and aerospace industry. Some composite structural work, sandwich panels and honeycomb panels were included. Some acoustic fatigue design characteristics for composite materials were developed by Wolf and Jacobson (3). A design guide was developed for some graphite epoxy structures by Holehouse (4), using the single-mode assumption, semi-empirical formulae established from a statistical analysis of a range of experimental tests. Multi-modal effects were observed, White (5), for aluminium alloys and CFRP plates.

The dynamic behaviour of isotropic and anisotropic panels subjected to both random acoustic excitation and in-plane compression was studied by Teh (6). In-plane compression effects in CFRP plates was studied by Galea (7) and the postbuckled behaviour of CRFP panels was investigated by Ng (8). The dynamic behaviour of clamped beam and plates under high sinusoidal excitation was investigated by Bennouna (9). The nonlinear mode shapes and natural frequencies of clamped-clamped beams and plates with sinusoidal excitation was studied by Benamar, Bennouna and White (10). The nonlinear multimode response of clamped rectangular aluminium plates subjected to random acoustic excitation was investigated by Wentz, Paul and Mei (11). The time domain Monte Carlo approach was investigated by Vaicatis (12). He showed an efficient use of this approach for the response analysis of nonlinear structures subjected to random pressure fields. Extensive work has been published on the stability analysis nonlinear beams and plates, such as a periodic solution of Duffing's equation published by Newland (13).

2.1 Nonlinear Considerations

Many researchers have investigated various forms of the Duffing equation with assumptions to suit their particular areas of interest. One example is the numerical perturbation method investigated by Nayfeh (14). Basic assumptions usually include single degree of freedom systems or multi-degree of freedom systems, free or forced vibration, harmonically or randomly excited, with or without damping and linear or nonlinear damping, and nonlinear stiffness types, such as cubic or higher orders. Some include weakly nonlinear systems. The focus of this effort was be multi-degree

of freedom systems, randomly excited with nonlinear damping and stiffness terms.

The identification of mathematical models to represent dynamic systems in general has attracted considerable attention in recent years. Identification of nonlinear systems ranges from methods simply to detect the presence or type of a nonlinear to those which seek to quantify the behaviour via some mathematical models. The force-state mapping approach proposed initially by Masri and Caughey (15, 16) stated that given an estimate for the system mass and measurements on estimates of the acceleration, velocity and displacement, the nonlinear restoring force is represented by a surface over the velocity-displacement plane and then a fit to the surface is carried out using an orthogonal Chebychev polynominal series expansion. An extension to multi-degree of freedom systems is possible.

Other researches (17-23) have focused development of the force-state mapping approach to the identification of nonlinear system. Particular attention was paid to the implementation of the curve fit to the restoring surface to where ordinary polynominal are superior to orthogonal polynominal, to the estimation of mass and to the location of the nonlinearity with a multi-degree of freedom system.

A starting point was to consider single channel analysis yielding power spectral densities and probability density functions. Transfer functions will be considered along with linear optimal filters, H_1 and H_2. The coherence functions, a measure of linearity, should yield useful information. Mathematical model tests under consideration are the Hilbert transform, coherency, non-Gaussian representation, higher transfer function tests, spectra spread and amplitude effects. Other possibilities include using the Volterra/Wiener functional series, identification of higher order transfer functions using bispectral analysis and parameter identification using nonlinear auto-regressive moving average models with exogenous inputs proposed by Billings et al (2,3,4). The above is considered a shopping list, since in depth analysis of many methods is not a practical consideration.

3.0 EXPERIMENTAL METHODS TO INVESTIGATE BEAMS AND PLATES AT LARGE DEFLECTIONS

3.1 Measurement Transducers

Various measurement transducers were tested to determine their suitability for beam and plate nonlinearity tests at high excitation levels. This requires linearity over the range of interest and large stand-off distances for displacement transducers to prevent the test specimen from contacting the transducer.

Displacement Transducers

Many displacement transducers are available from manufacturers and some developed by specialists such as ISVR. To achieve five beam thicknesses of dynamic displacement, using a 2 mm beam would require 10 mm peak-to-peak. Also, a non-contacting device was desired to prevent mass loading the vibrating surface and to avoid attachment problems. Another consideration was the cost per channel for the measuring devices.

3.1.1 Optical Vibration Transducers (OVT)

Optical vibration transducers were developed at ISVR by Wright (24). The arrangement of the light source and the sensing photocell is shown in Fig. 1. The intensity of the light incident on a photocell at the observation point is proportional to the distance between the cell and the vibrating surface.

Dynamic calibration tests of an ISVR OVT were made with a clamped aluminium beam as shown in Fig. 2. Large deflections were obtained at 30 and 76 Hz resonant frequencies. A travelling microscope was used to measure the displacements for the output voltage of the OVT after modifying the high bypass filter changing the low cut-off frequency from 30 Hz to 3 Hz. The results are shown in Fig. 3 and the modified electronic circuit OVT filter is shown in Fig. 4. The calibration curve looked somewhat linear, however, static measurements shown in Fig. 5 indicated that for large deflection measurements, up to 40 mm, the calibration curve was not linear. The output voltage was dependent upon the distance the OVT sensor head was from the vibrating surface. An electronic compensating circuit was investigated along with possible correction methods to the data; however, further development time will be needed for pursuing this problem.

3.1.2 Fibre Optical Methods

Fibre optical methods were considered for the beam tests. Dr. Redman-White (25) at ISVR developed a prototype using a bundle of fibers. The linear range was considered to be too small. Other investigators, Mohanan et al (26), have developed such devices; however, the distance from the fibre optic source and the photodetector was 0.5 mm which was too small. The device used a tungsten halogen lamp detected by a position sensitive differential photodetector, modulated by sinusoidal excitation. Further consideration of fibre optical measurement devices was postponed.

3.1.3 Laser Vibrometers

The ISVR developed laser vibrometer did not have sufficient range to measure the beam displacements up to the desired level. Wave distortion was apparent at relatively low displacement levels. A B&K. laser Vibrometer model no. 3544 was checked with a clamped beam arrangement. Up to 20 mm peak-to-peak displacements were obtained before reaching the limit of the instrument. The first coil magnet after modification also was limited to 20 mm peak-to-peak displacements due to the coil length and the width of the permagnet pole pieces. The vibrometer was checked against a B&K Type 4344 accelerometer with good agreement on the displacement and velocity scales. Although the vibrometer may be an expensive device, good results were obtained as shown in section 3.6.

3.1.4 Accelerometers

Displacement curves of the beams were measured with accelerometers, B&K Type 4344 or equivalent (2 grammes) along with charge amplifiers, B&K Type 2635. Direct attachment of a mass to the vibrating surface affects the mass of the vibrating system which can change the response of the system slightly when the relative mass of the accelerometer is small compared with the mass of the beam. The major disadvantage of this method is the attachment methods to the beam. Wax was used quite successfully for displacement as large as 3.0 mm peak-to-peak. Details of the test set-up are described in the appropriate section for each test.

3.1.5 Other Displacement Transducers

Other devices using ultrasonic devices and infra-red devices were inexpensive and looked promising. Ultrasonic devices tested reached one phase shift in about 2 mm which was too small. Methods of multiple phase shifting were

considered, but needed further development. Linear Variable Differential Transforms (LVDT) and eddy current devices investigated also had insufficient range. Coil magnet transducers are relatively inexpensive. They were considered worthwhile for investigation. The coil was attached to the vibrating surface and an annular permagnet was fixed to the test rig. Motion of the coil in the magnetic coil produces a current proportional to the displacement of the coil. This approach was tried on the clamped beam test rig with some spare coils, circuits and magnets. The arrangement and test results are shown in Fig. 6 with a 40.5 cm aluminium beam clamped. An accelerometer was mounted on the opposite face of the beam as the coil magnet transducer. Favorable results were obtained. A more practical coil was designed and built with a large displacement capability of 20 mm peak-to-peak. The design of the transducer is shown in Fig. 7. The aluminium wound coil mass is only 1.67 gm compared to a small B&K accelerometer such as the type 4344 which has a mass of 2 gm. The new coil magnet transducer was not tested due to time constraints.

3.2 Strain Gauges

Suitable strain gauges were readily available and relatively inexpensive. Temperature compensating gauges for aluminium were selected. A gauge length of 1 mm was selected for low mass loading and small enough to reach close to the clamping frame or clamping block for both panel and beam tests. Temperature compensation was built into the gauge by the manufacturer by using a backing material suitable for the material attached. The gauges were made by Tokyo Sokki Kenkyujo Co. Ltd., type FLE-1-23, gauge resistance was 120±0.3 ohms, gauge factor 2.19, lot no. 355211.

3.3 Microphones

The microphones used in the progressive wave tunnel were 1/2 inch B&K type 4133 and 4134. A B&K pistonphone type 4220 was used to calibrate the microphone channels.

3.4 Coil Magnet Shakers

Various arrangements of voice coils and annular permanent magnets are available which are relatively inexpensive and have no suspension system between coil and magnet assembly. This type of shaker was utilized rather than commercially available shakers with shake tables flexurally mounted. A rather large, 13.7 cm diameter magnet was selected for test. A 4.9 kg mass was suspended on light wire rope to provide a hanging mass to determine the force of the coil magnet exciter as a function of current. The mass was suspended in a steel frame arrangement. The test

arrangement is shown in Fig. 8.

Preliminary tests of the coil magnet driving a 4.9 kg suspended mass indicated some nonlinear behaviour with different sinusoidal frequencies and random excitation. The force versus frequency characteristics were not linear over the frequency range of interest as shown in Fig. 9. The permanent magnet was modified as shown in Fig. 10 to improve its flux characteristics and linearity. The coil assembly was reinforced with graphite-epoxy to make it stiffer; however, the original mass was increased from 13.3 g to 19.2 g after reinforcement. Sinusoidal and white noise signals (filtered) were used to drive the coil. At low sinusoidal frequencies (0 - 5 Hz) the mass tended to traverse laterally with large coil movements. These frequencies were avoided to prevent damage to the coil. Ringing noise of the mass was quite noticeable by ear especially in the range of 1000 - 1300 Hz. The mounting rig also resonated at 552, 811 and 894 Hz. The force showed an increasing trend with increasing current, especially around 1000 Hz and above as shown in Fig. 11. The sine signal showing some high frequency ripple on the periodic signal at 1000 Hz. The current was adjusted when necessary to maintain constant current measurements.

Weights were added to the support frame to raise the resonance frequencies above those of interest. The calibration curves for sinusoidal excitation are shown in Fig. 11 and for random excitation in Fig. 12. The small amount of nonlinear response at higher frequencies was attributed to the ringing of the solid steel cylindrical mass.

3.5 Constant Current Modifier

Since the force applied to a beam with a shaker is directly proportional to the current through the coil, it is desirable to keep the current relatively constant over the frequency range of interest. Both sinusoidal and random excitation were used in the beam tests with large variations in coil current at especially at the first resonant frequency. With the help of ISVR's Electronic Shop a "constant current modifier" electronic circuit was developed to minimize the current reduction at resonance as shown in Fig. 13. The test set-up for the beam experiments is shown in Fig. 14. The beam experiments are described in the next section and the results are discussed on the following section.

Transfer functions can be utilized to minimize the effects of the force function varying with frequency rather than remaining constant over the frequency range of interest. This can be accomplished by dividing the output (response) spectrum by the input spectrum. Measurement inaccuracies with large changes at resonance frequencies and phase shifting can result in some inaccuracies. These

techniques are based upon linear assumptions including reciprocity. Investigation of nonlinear beam and plate behaviour requires linear instrumentation and data processing techniques. The meaning of transfer functions and coherence at high levels of excitation is not clear. One of the tests for nonlinearity is variations in reciprocity. The more variations removed from the force input was considered worthwhile to minimize errors in data processing.

3.6 Clamped Aluminium Beam Experiments

Beams with various boundary conditions were considered for investigation. The clamped-clamped (C-C) beam arrangement was selected. All beams utilised in these experiments were aluminium DTD 5070 (DURAL) and the sizes were all 2 x 20 x 630 mm. For the C-C case, the distance between supports was 405 mm. The mass of three different beams varied from 72.9 to 75.0 g. Beam 1 (7.13 g) was painted lightly with white paint to provide a good light reflective surface and to reduce the effects of other light sources in the laboratory. A strain gauge and lead wire were also attached which was included in the mass. Tests with this beam utilized an aluminium "c" clamp arrangement with a plastic screw shown in Fig. 10 to attach the force coil to the beam at various locations. The mass of the clamp and plastic screw were 9.34 g and 0.343 g respectively. Beam 2 contained six strain gauges and a plastic screw adhesively bonded to the center of the beam and a plastic nut for a total mass of 75.0 g. The mass of the strain gauges and lead wires were negligible. The strain gauge plan is shown in Fig. 15.

Preliminary tests including displacement transducer evaluations were performed on the test rig shown in Fig. 16 and 17 similar to that used by Bennouna(9). The beam was clamped on two heavy steel blocks bottled to a heavy concrete base vibration isolated on cork pads. Clamping aluminium with steel mountings can provide buckling in beams or plates with only a few degrees temperature change in the laboratory environment due to the large difference between the thermal coefficients of expansion between the two materials. Laboratory temperature measurements were made each day that tests were performed. An axial loading block was installed to apply different amounts of axial tension to the beams. The travelling microscope tests to calibrate dynamically the OVT were carried out using part of the rig to support a cantilever beam.

3.6.1 Results of the Clamped-Clamped Beam Tests With the Movable Coil Clamp

Different levels of random excitation bandpassed filtered from 10 to 1000 Hz at coil currents of 0.25, 0.35 and 0.5 amperes are shown in Figures 18, 19

and 20 respectively along with the displacements measured with an accelerometer at the center of the beam. The fundamental bending mode at 47 Hz increased with increasing excitation level. Fig. 21 shows the velocity response of the beam excited by 0.5 amperes and Fig. 22 shows the acceleration response. Without the current modifier, the spectrum of the excitation dips considerably at the fundamental beam response as shown in Fig. 23 and 24 and the displacement peak decreases considerably.

3.6.2 Results of the Clamped-Clamped Beam Tests With the Coil Attached to the Center of the Beam

Displacement measurements were obtained using a laser velocimeter on beam 2 with the strain gauges installed. No axial tension was placed on the beam. No appreciable amount of strain was noted after clamping the beam in place. Strain measurements were noted before and after the displacement measurements and no appreciable strain was observed. Three displacement measurements at 15 locations along the length of the beam were made at three different levels of sinusoidal excitation as shown in Fig. 25. The normalized displacements are shown in Fig. 26. Sinusoidal frequency sweeps at very low rates were made from below resonance increasing in frequency and from above resonance, decreasing in frequency. Two levels of excitation were used as shown in Fig. 27. The jump phenomena were observed with a large drop in amplitude for a small increase in frequency. The fundamental resonant frequency changed from as low as 42 Hz to 63 Hz. No slippage was apparent upon close examination of the beam ends for wear markings, removing the beam after testing. The random tests were performed later when a PC data acquisition capability was available.

3.6.3 Simply Supports Beam Considerations

The simply supported boundary conditions for a beam were considered. Immoveable end restraints were considered essential for nonlinear behaviour due to the large membrane strains expected. Various schemes to prevent motion in three directions while permitting frictionless rotation of the ends of the beam were considered. Low friction pinned arrangements are shown in Fig. 28, 29 and 30, but were considered too costly to make and beyond the force capability of the coil magnet shaker being utilised. A ball bearing approach allowing low frictional rotation of the beam ends was considered. However, a considerable amount of mass on both ends would be needed around the pivot points and changes in the cross-sectional area around the ends were considered undesirable. The final approach used shims or membranes permitting fairly rigid restraint in three directions while allowing the beam to rotate with very little resistance. Preliminary design ideas were considered, but

fabrication cost and time resulted in postponing the idea. Flexible boundary conditions were considered more closely related to aerospace structure. One design is shown in Fig. 31, but postponed for consideration later.

3.6.4 Statistical Analysis of Test Data

The statistics of instantaneous amplitudes of random noise were investigated using DATS on VAX and PC DATS at ISVR. For a narrow band of random noise, the probability density has the well known bell shape curve which corresponds to a Gaussian or normal probability distribution. Attempts to use the probability density function in the probability analysis packages for both systems produced confusing results. Attempts starting with a random signal internally generated on a PC were also confusing, since a Gaussian distribution was not obtained. The problem was eventually solved with the help of the Data Processing Group. It was traced to the method of generating the random signal. A new method was developed where no repetitions were encountered over the entire time history and amplitudes were not clipped. Examples of the time history are shown in Fig. 32 and 33. The probability distribution obtained from the time history is shown in Fig. 34.

3.7 Panel Tests in Progressive Wave Tube (PWT)

The PWT of rectangular cross-section (304.8 x 609.6 mm) (1 ft x 2 ft) with a 30 Kw Wyle WAS 3000 air modulator was used to perform both sinusoidal and random plate tests as shown in Fig. 35. The tunnel side was blocked with a plywood panel to obtain the acoustic characteristics at four microphone locations. The microphones were orientated for grazing incidence. Adjustments were made to the 1/3 octave band filter set to yield a relatively flat power spectral density (PSD). The spectrometer used produced outputs between 0 and 100 volts; whereas, the PC data acquisition system was limited to 1 volt. A four channel voltage reducer was designed and built by the ISVR Electronic Shop to remedy this problem.

3.7.1 Results of Panel Tests in PWT

Examples of time histories obtained with four microphones are shown in Fig. 36. All four microphones were within a 2 dB overall range. The corresponding power spectral densities (PSD) are shown in Fig. 37. The data from the downstream position was not good, since the 50 Hz mains noise was predominant. A comparison of two levels is shown in Fig. 38. A relatively flat spectrum shape was obtained between 100 and 500 Hz. An example of a 1/3 octave band input to the air modulator and the spectrum obtained at microphone no 1 is shown in Fig. 39. The 1/3 step increase per 1/3 octave yields a flat spectrum using a 1 Hz bandwidth.

A flat rectangular aluminium plate L71 18 SWG was instrumented with 10 strain gauges. Pairs of strain gauges were mounted back-to-back as shown in Fig. 40. Edge gauges 2 and 7 were located for maximum strain for the first mode response. Edge gauges 1 and 6 were located for the third mode response. The back-to-back arrangement was selected to measure bending strain only or axial (tension) strain only by changing the wiring connection on the Weathstone bridges used. The aluminium plate and steel frame were heated from 23°C to 37°C before torquing the bolts clamping the plate to the frame. This provided a light tension to the panel as long as the environment did not exceed 37°C. There was sufficient hole clearance space to prevent the panel from buckling when heated. The panel frame was suspended by two chains in the plywood opening in the side of the duct as shown in Fig. 41. A sponge rubber gasket sealed the panel frame in the plywood rectangular opening. First tests with the panel installed resulted in the panel slipping out of the opening at the bottom. Corner blocks with foam damping were installed in the corners to keep the panel frame in place.

A few examples of the power spectral densities with random excitation at low levels are shown in Fig. 42 and 43. The voltage readings were not adjusted to reflect the true gain settings.

4.0 Conclusions

Many acoustic fatigue investigations have been made over the years and many publications are available. Nonlinear aspects of beams and plates excitated at high levels were investigated. Although it is too early to conclude much about the beam and plate test results, a few observations will be made. Multimode response, especially with plates is evident as well as the jump phenomena. Data processing methods need careful investigation to prevent meaningless data from confusing the evaluation. Further development of theoretical mathematical models is needed for specific nonlinear problems.

5.0 References

1. A.G.R. Thomson, R.F. Lambert, "Acoustic Fatigue Design Data," AGARDOGRAPH 162, 1973.

2. F.F. Rudder, H.E. Plumblee, "Sonic Fatigue Design Guide for Military Aircraft," AFFDL-TR-74-112, May 1975.

3. N.D. Wolf and M.J. Jacobson, "Design and Sonic Fatigue Characteristics of Composite Material Components," AGARD Conference Proceeding No 113, 1972.

4. I. Holehouse, "Sonic Fatigue Design Technique for Advance Composite Aircraft Structures," AFWAL-TR-80-3019, WPAFB, Ohio April 1980.

5. R.G. White, "Comparison of Statistical Properties of the Aluminium Alloy and CFRP Plates in Acoustic Excitation. J. Composites," October 1978 p. 251-258.

6. C.E. Teh, "Dynamic Behaviour and Acoustic Fatigue of Isotropic and Anisotropic Panels Under Static In-Plane Compression and Acoustic Excitation," PhD Thesis, 1981, University of Southampton, UK.

7. S.C.P. Galea, "Effects of Temperature on Acoustically Induced Strains and Damage Propagation in CFRP plates," PhD Thesis, 1989, University of Southampton, UK.

8. C.F. Ng, "Dynamic Behaviour of Postbuckled Composite Plates Under Acoustic Excitation," PhD Thesis, 1989 University of Southampton, UK.

9. M.M. K. Bennouna, "Nonlinear Behaviour of a Clamped-Clamped Beam with Consideration of Fatigue Life," PhD Thesis, 1982 University of Southampton, UK.

10. R. Benamar, M.M.K. Bennouna, R.G. White, "Non-linear Mode Shapes and Natural Frequencies of Fully Clamped Beams and Plates," Proc of the 7th International Modal Analysis Conference, Las Vegas, 1989.

11. K.R. Wentz, D.B. Paul, and C. Mei, "Large Deflection Random Response of Symmetric Laminated Composite Plates," Bulletin 52, Teh Shock and Vibration Information Center, Naval Research Laboratory, Washington DC, USA pp 99-110.

12. R. Vaicatis, S. Choi, "Sonic Fatigue and Nonlinear Response of Stiffened Panels," AIAA 12th Aeroacoustic Conference, April 10-12, 1989, San Antonio, TX, USA, AIAA 89-1101.

13. D.E. Newland, Mechanical Vibration Analytical Computation, Longman Scientific and Technical, John Wiley & Sons, 1989 p 450-457.

14. A.H. Nayfeh, D.T. Mook, D.W. Lobitz., "Numerical-Perturbation Method for the Nonlinear Analysis of Structural Vibrations," AIAA Journal Vol 12, No 9, Sept 1974.

15. S.F. Masri and T.K. Caughey, 1979 Journal of Applied Mechanics 46, pp 433-447 "A Non-Parametric Identification Technique for Nonlinear Dynamic Problems".

16. S.F. Masri, H. Sassi and T.K. Caughey., 1982 Journal of Applied Mechanics 49, pp 619-627. "Non-Parametric Identification of Nearly Arbitrary Nonlinear Systems".

17. E.F. Crawley and A.C. Aubert., 1986 AIAA Journal Vol 24, pp 155-162. "Identification of Nonlinear Structural Elements by Force-State Mapping".

18. K.J. O'Donnell and E.F. Crawley. MIT Space System Laboratory Report. SSL 16-85. "Identification of Nonlinear System Parameters on Space Structure Joints Using the Force-State Mapping Technique".

19. K. Worden and G.R. Tomlinson., 6th IMAC 1988, pp 1471-1479. "Developments in Force-State Mapping for Nonlinear Systems".

20. K. Worden and G.R. Tomlinson, 7th IMAC 1989, pp 347-1351, "Application of the Restoring Force Surface Method to Nonlinear Elements".

21. M.A.Al-Hadid and J.R. Wright., "Developments in the Force-State Mapping Technique for Nonlinear Systems and the Extension to the Location of Nonlinear Elements in a Lumped Parameter System". Accepted for Publication to the Journal of Mechanical Systems and Signal Processing.

22. N.F. Hunter, T.Paez and D.L. Gregory., 7th IMAC 1989, pp843-849. "Force-State Mapping Using Experimental Data".

23. Y. Yaang and S.R. Ibrahim. Journal of Vibration, Acoustic Stress and Reliability in Design, Vol. 107, pp 60-66. "A Non-Parametric Identification Technique for a Variety of Discrete Nonlinear Vibrating Systems".

24. G.G. Wright, "The Dynamic Properties of Fibre Reinforced Plastic Beams," ISVR Technical Report No. 51, University of Southampton, U.K. (1971).

25. W. Redman-White, "The Measurement of Structural Wave Intensity," PhD Thesis, University of Southampton, U.K. (1983).

26. V. Mohanan, B.K. Roy and V.T. Chitris, "Calibration of Accelerometers by Use of an Optical Fibre Vibration Sensor," Applied Acoustics 28, 95-103 (1989).

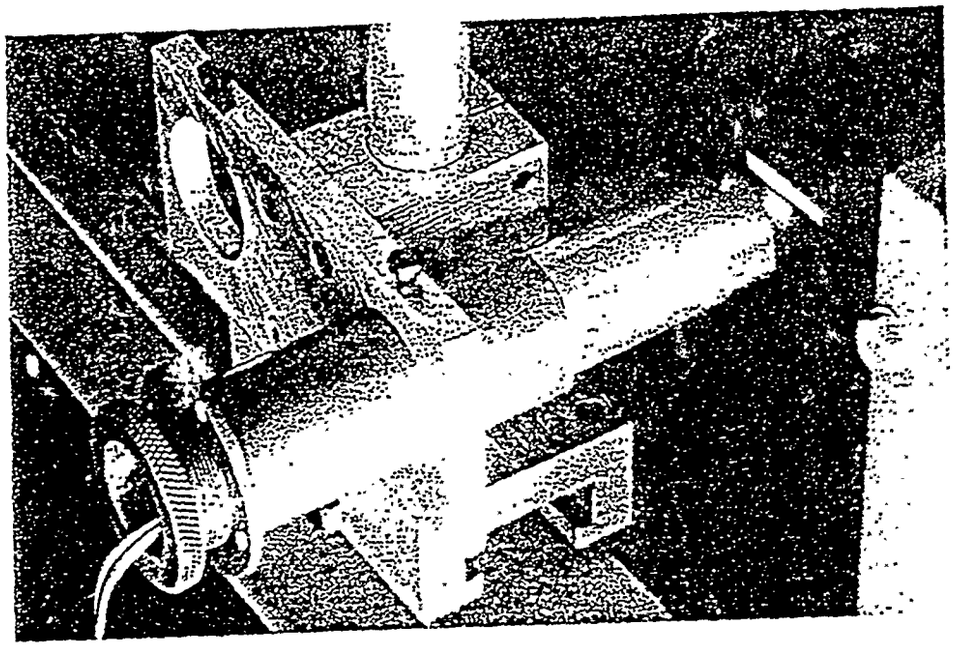

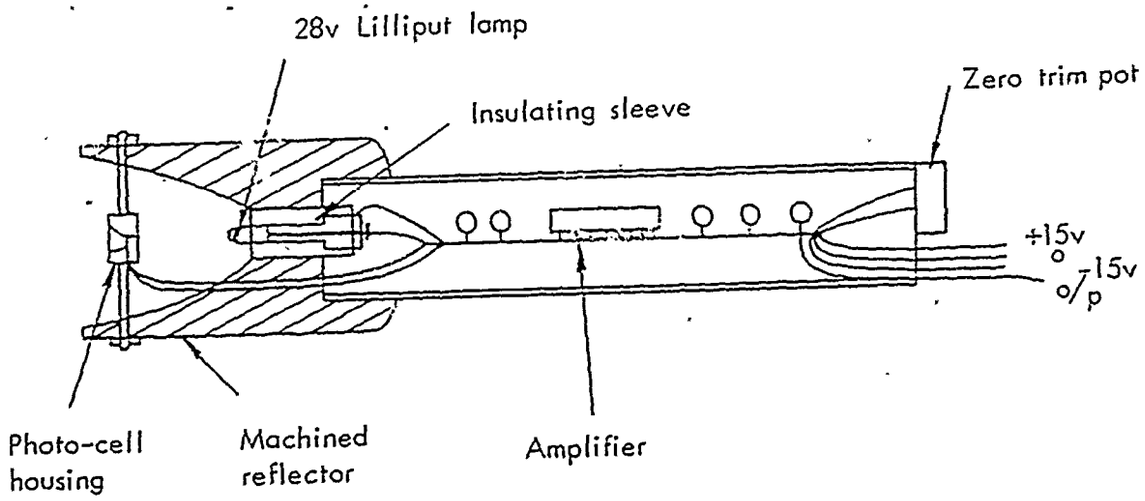

FIG 1: DETAILS OF THE O.V.T. TYPE B

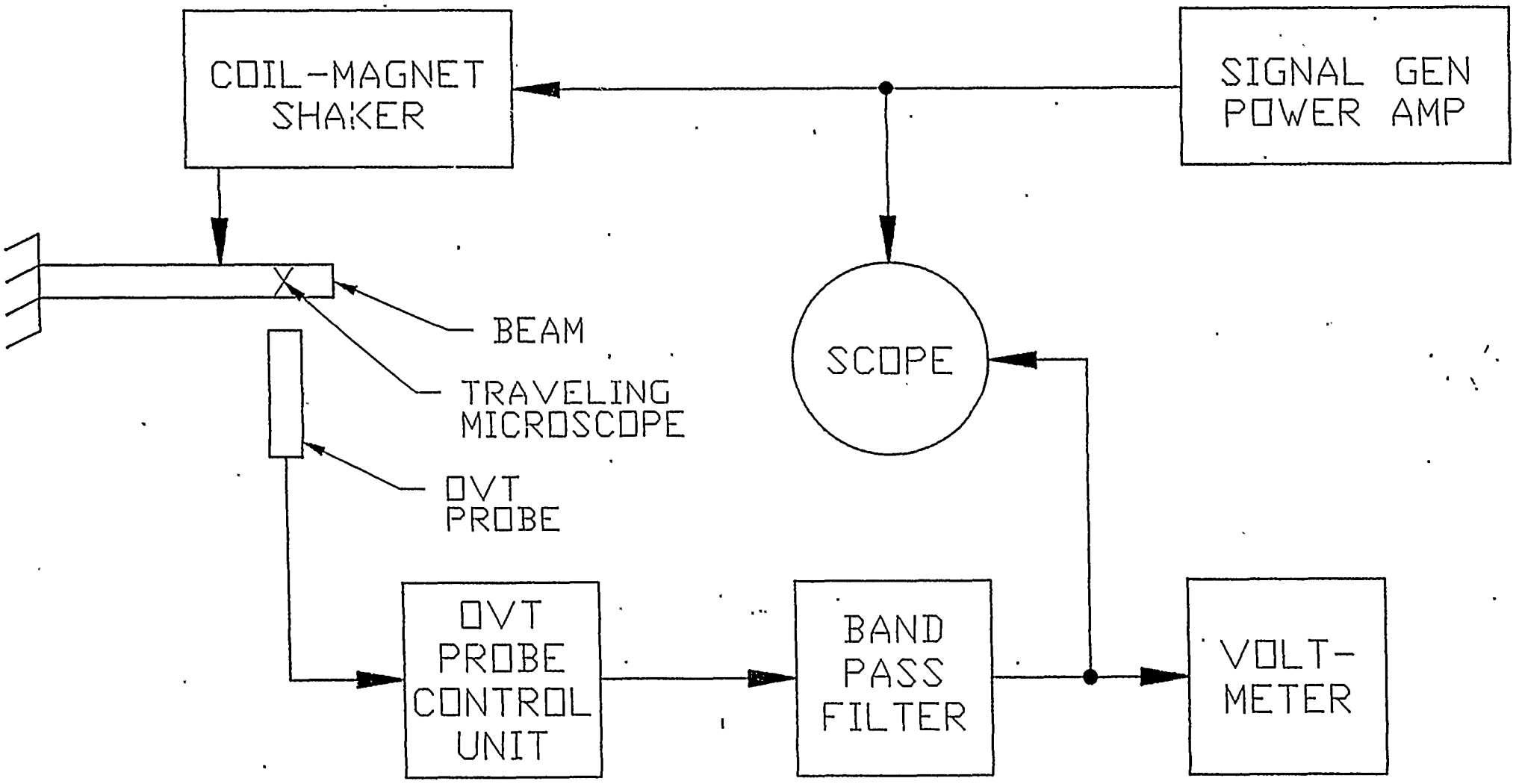

BEAM: 315mm
OVT: 293mm
SHAKER: 130mm
OVT PROBE DIA.: 30mm

FIGURE 2: CANTILEVER BEAM OVT CALIBRATION TEST CONFIGURATION

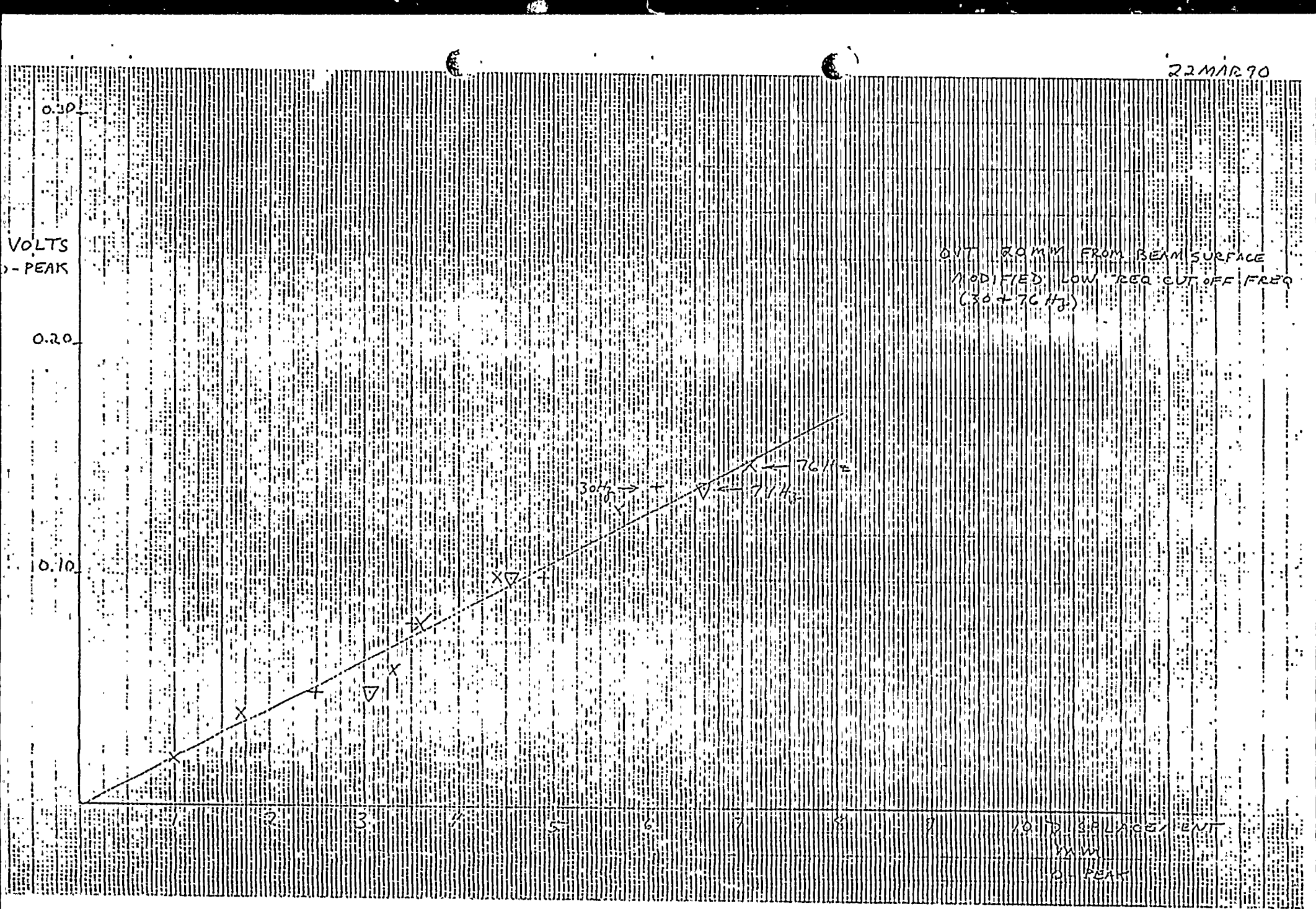

FIGURE 3: OVT TRAVELING MICROSCOPE MEASUREMENTS AT 30, 74, AND 76 Hz

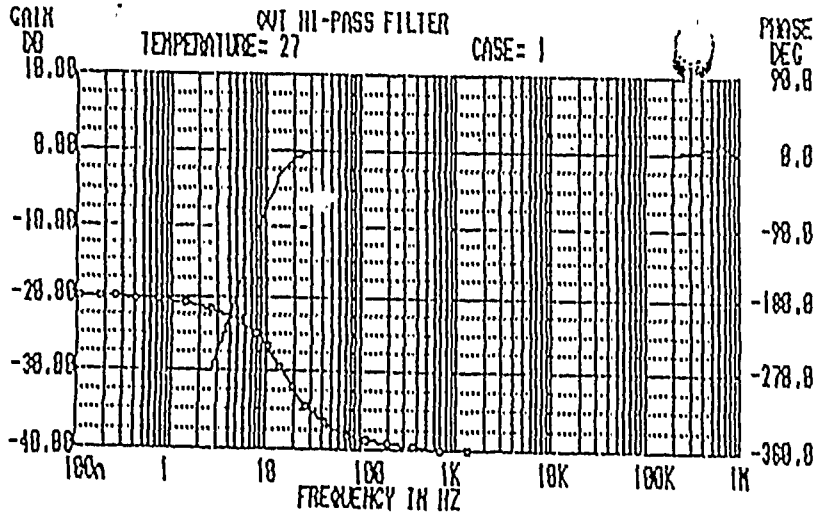

Frequency = 100.0000104 HZ Gain = -0.025 DB
Phase angle= -450.094 Degrees Group delay= 0.0000100 Sec
Gain slope = -217.7341E-02 DB/OCT Peak gain = 1.2280B/F= 671.1207501B3

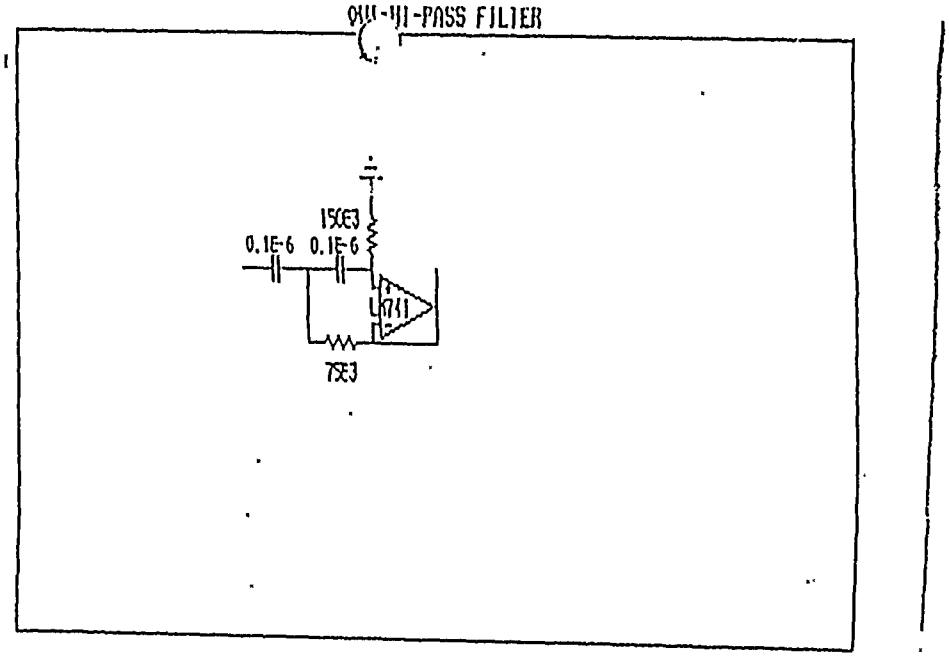

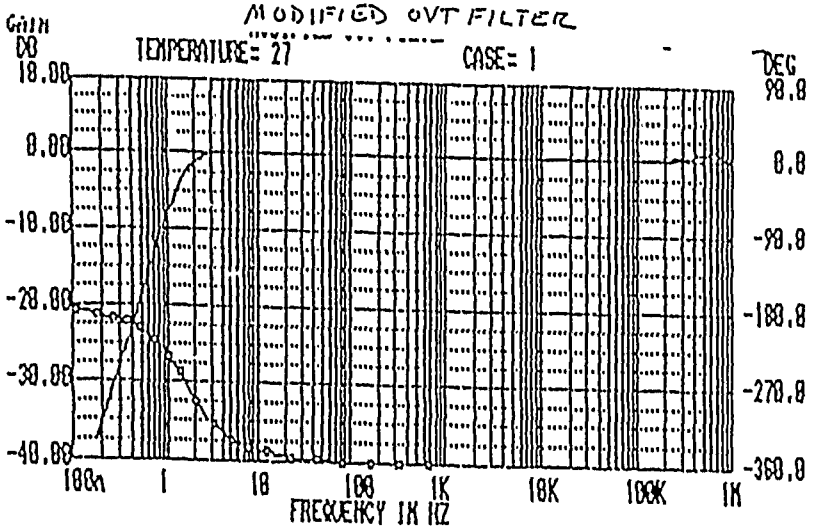

Frequency = 100.0000104 HZ Gain = -0.025 DB
Phase angle= -450.896 Degrees Group delay= 0.0000100 Sec
Gain slope = -217.7179E-02 DB/OCT Peak gain = 1.2280B/F= 671.0912701B3

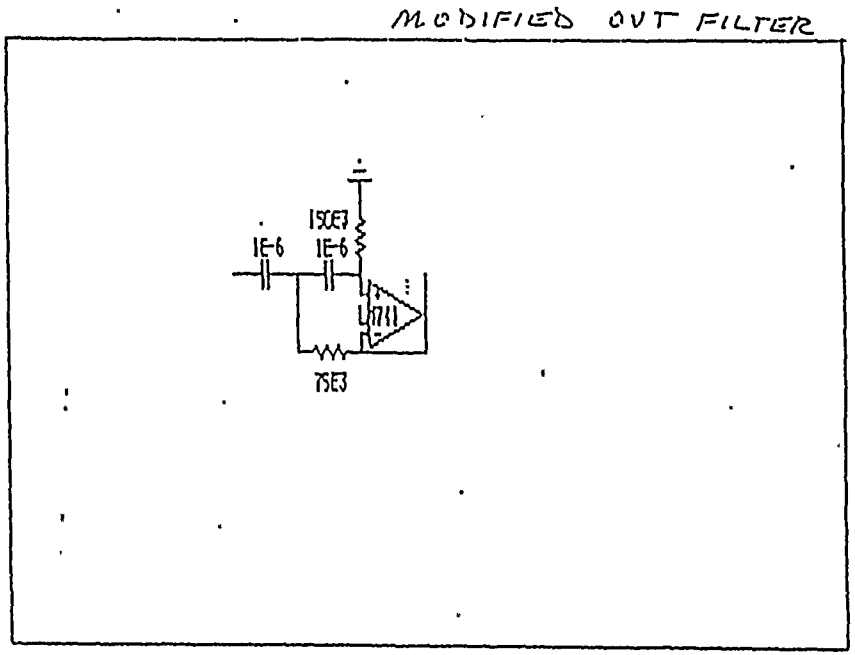

FIGURE 4: MODIFICATIONS TO OVT CIRCUIT

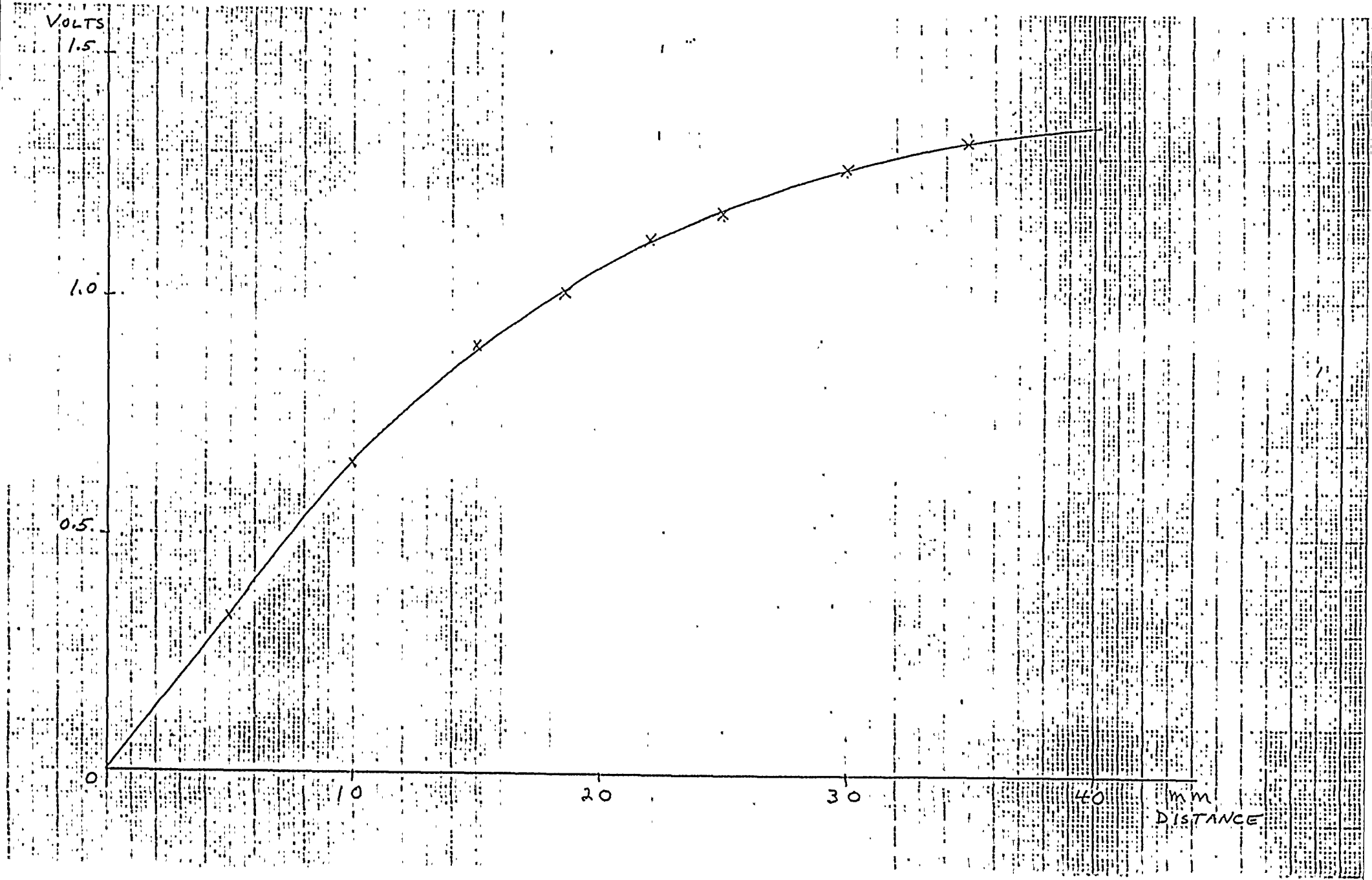

FIGURE 5: STATIC DISPLACEMENTS FOR OVT

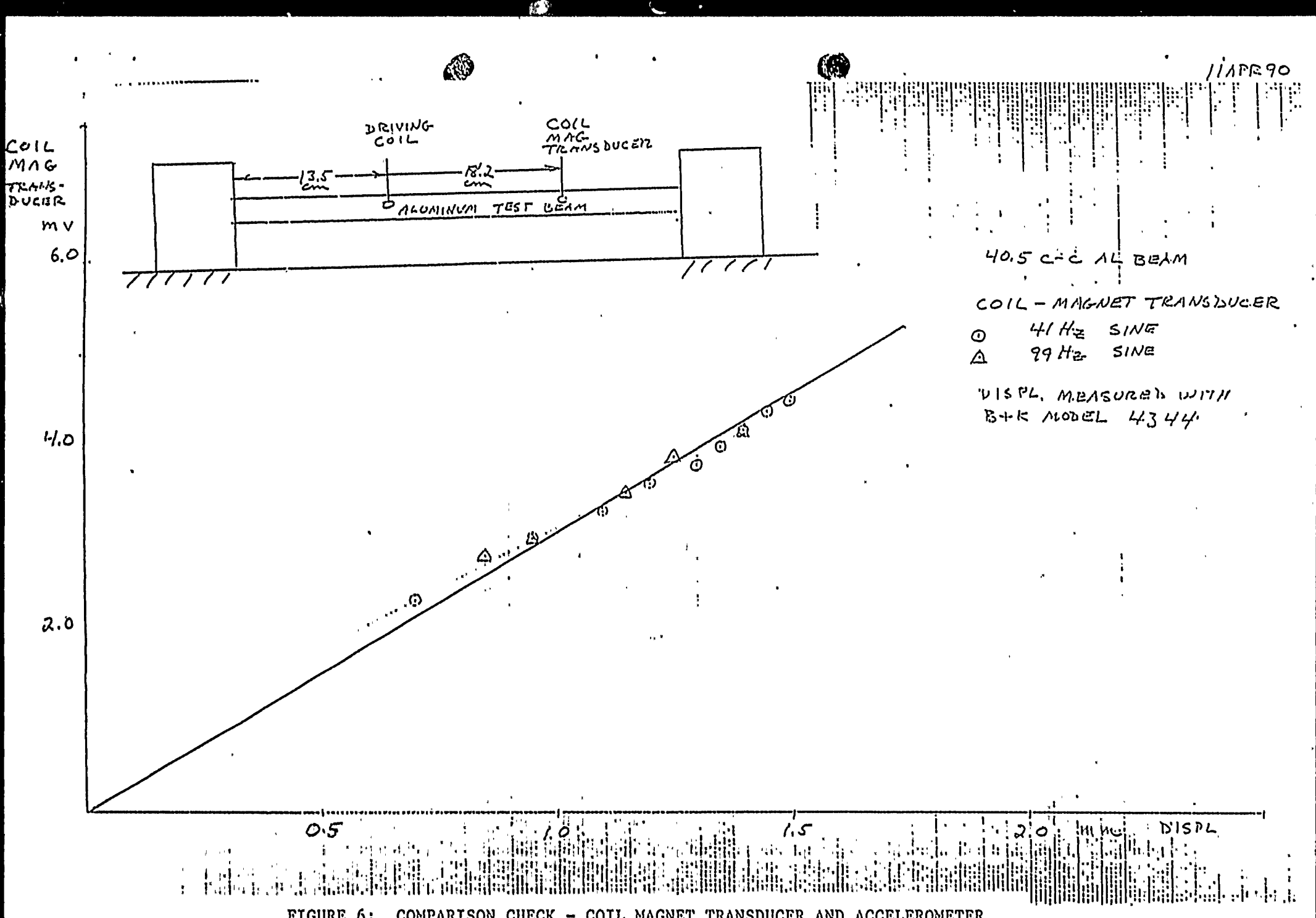

FIGURE 6: COMPARISON CHECK - COIL MAGNET TRANSDUCER AND ACCELEROMETER

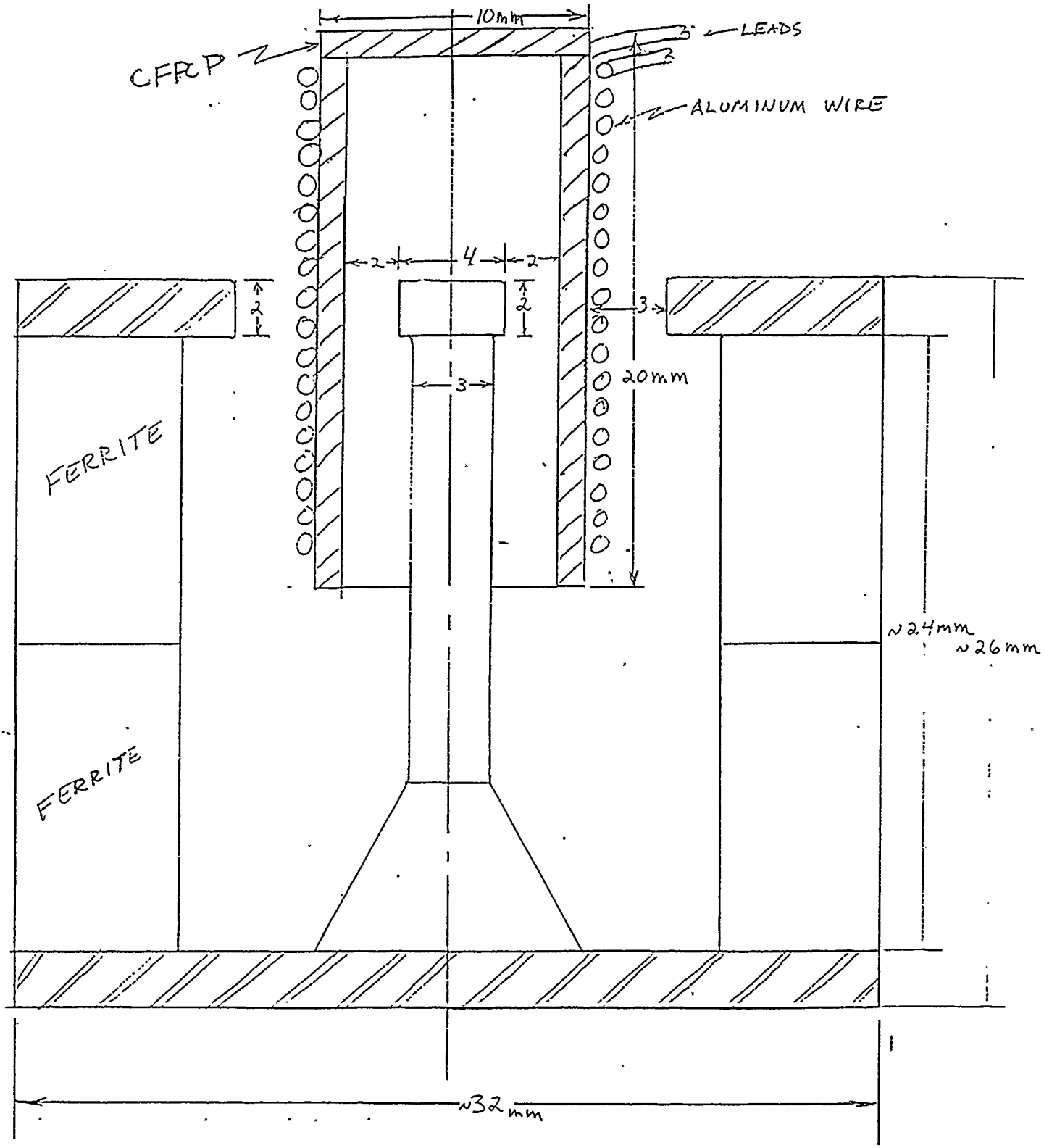

FIGURE 7: COIL MAGNET TRANSDUCER

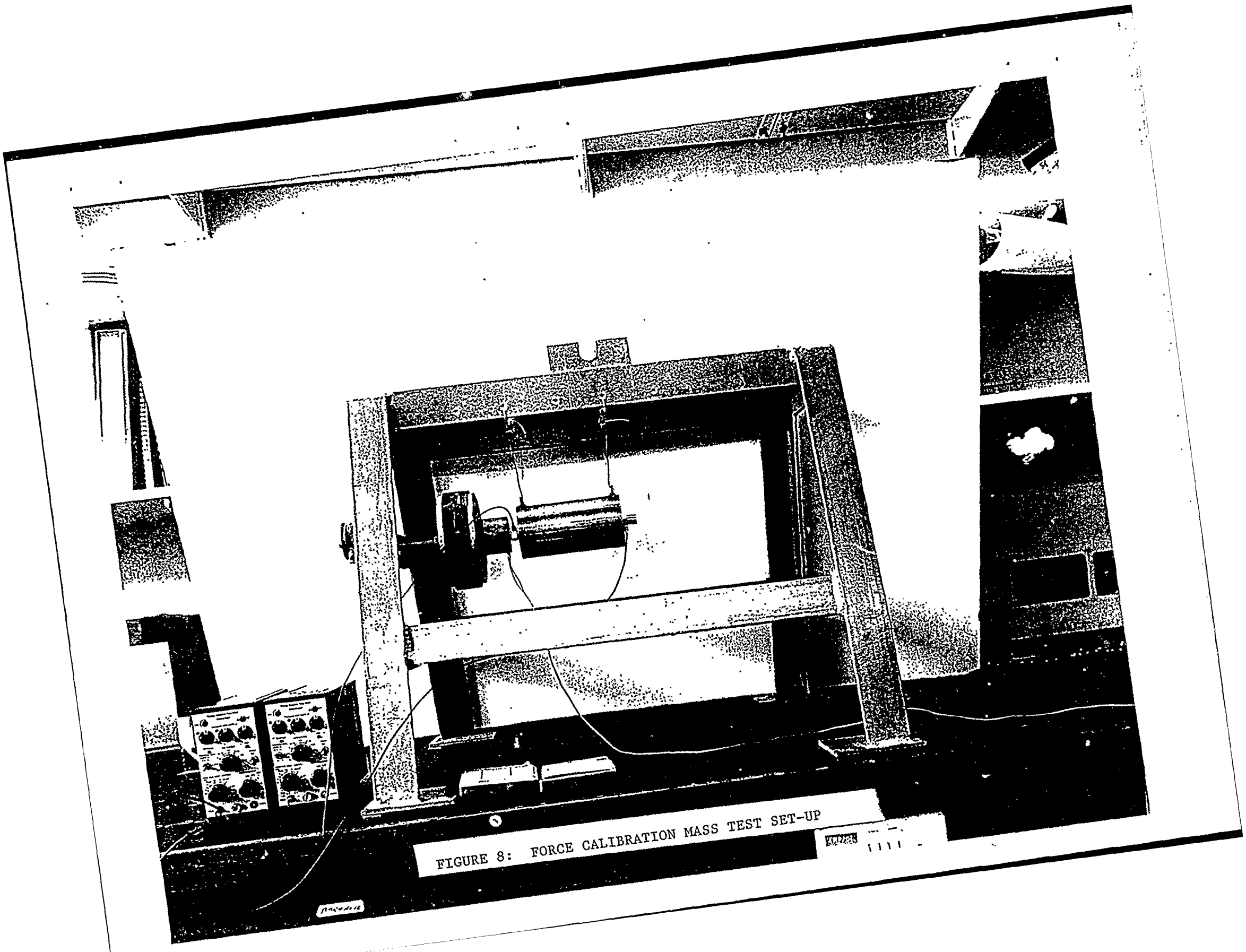

FIGURE 8: FORCE CALIBRATION MASS TEST SET-UP

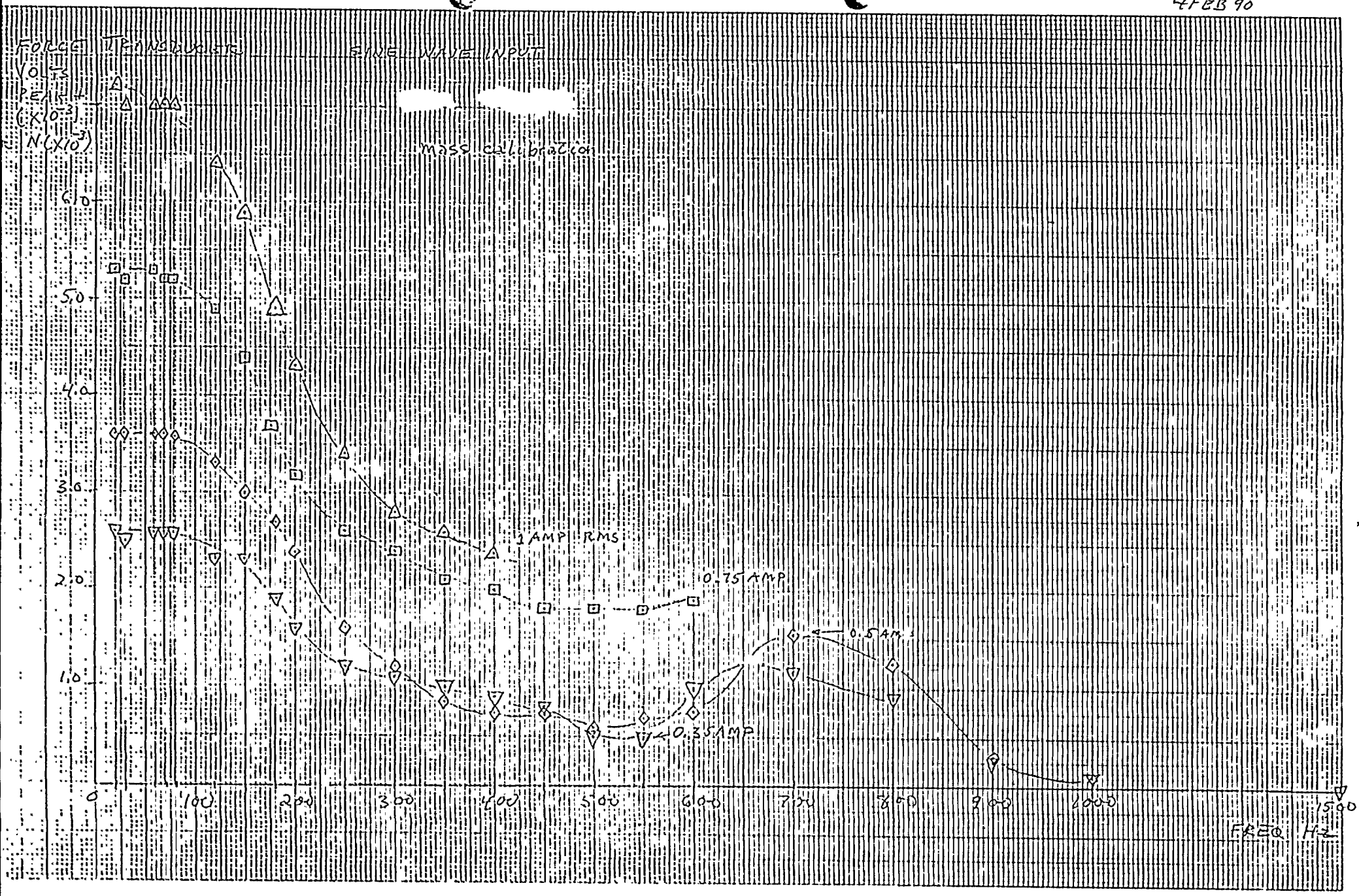

FIGURE 9: FORCE VS FREQUENCY CHARACTERISTICS OF COIL MAGNET

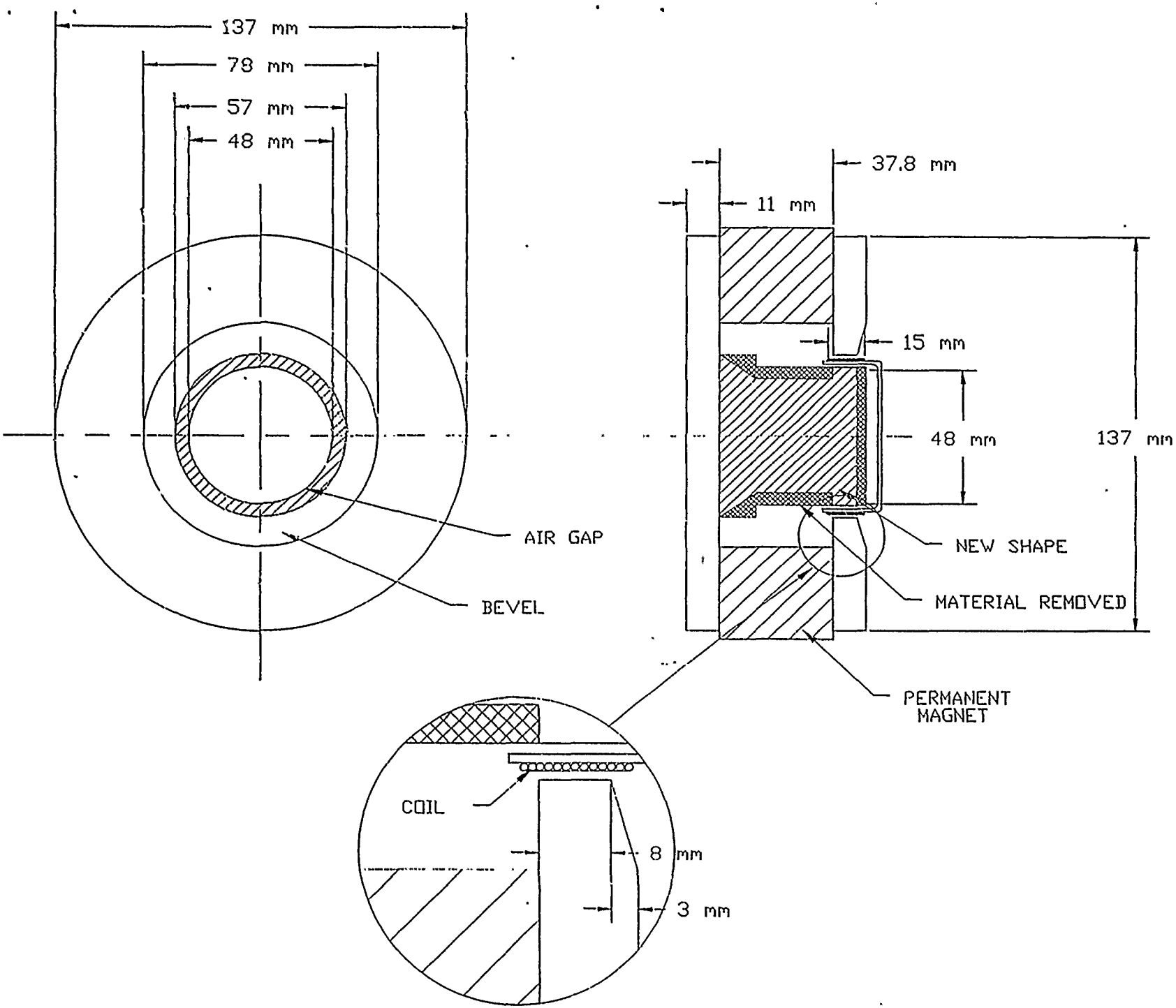

FIGURE 10: COIL MAGNET EXCITER ASSEMBLY

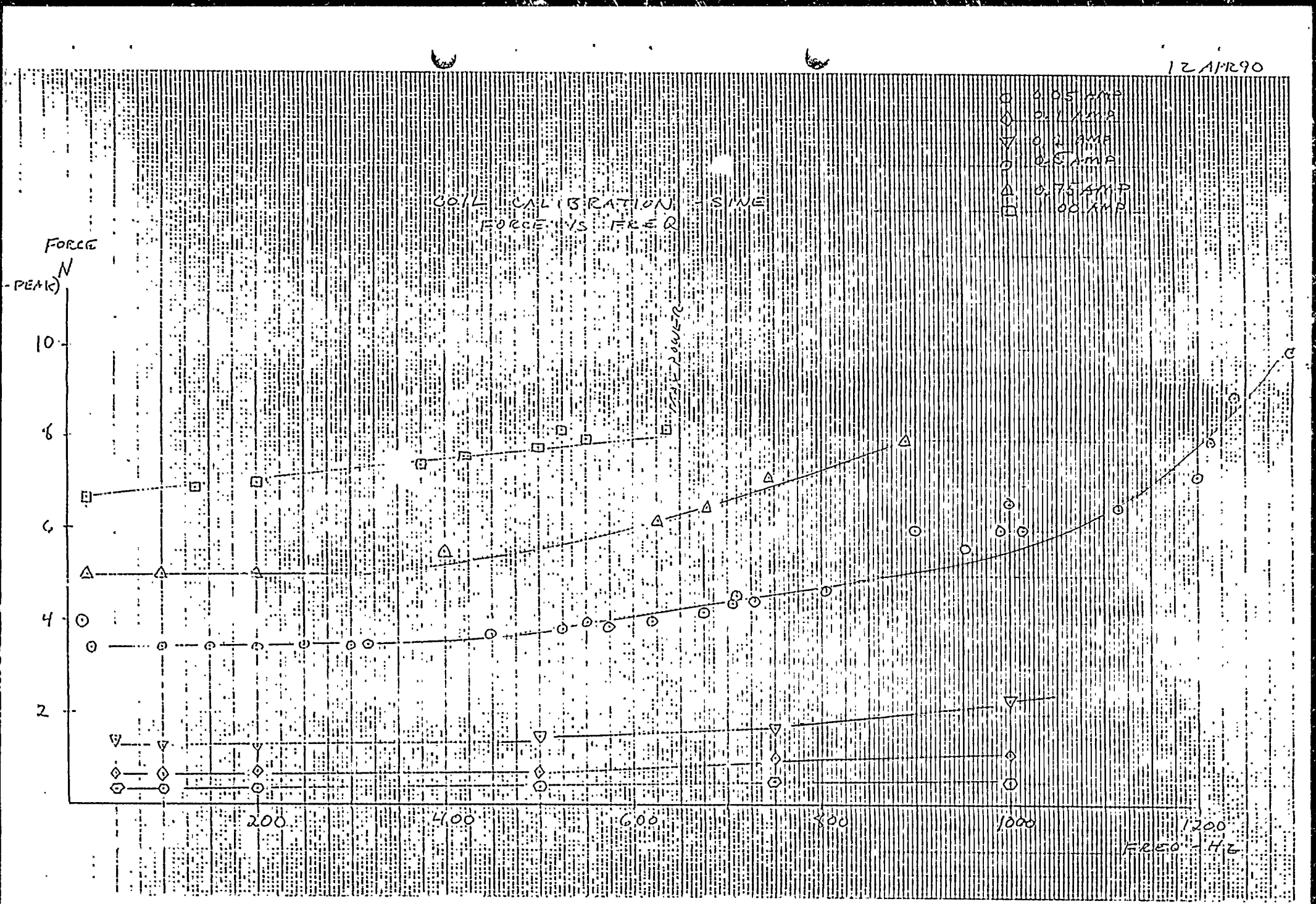

FIGURE 11: COIL CALIBRATION - SINUSOIDAL EXCITATION

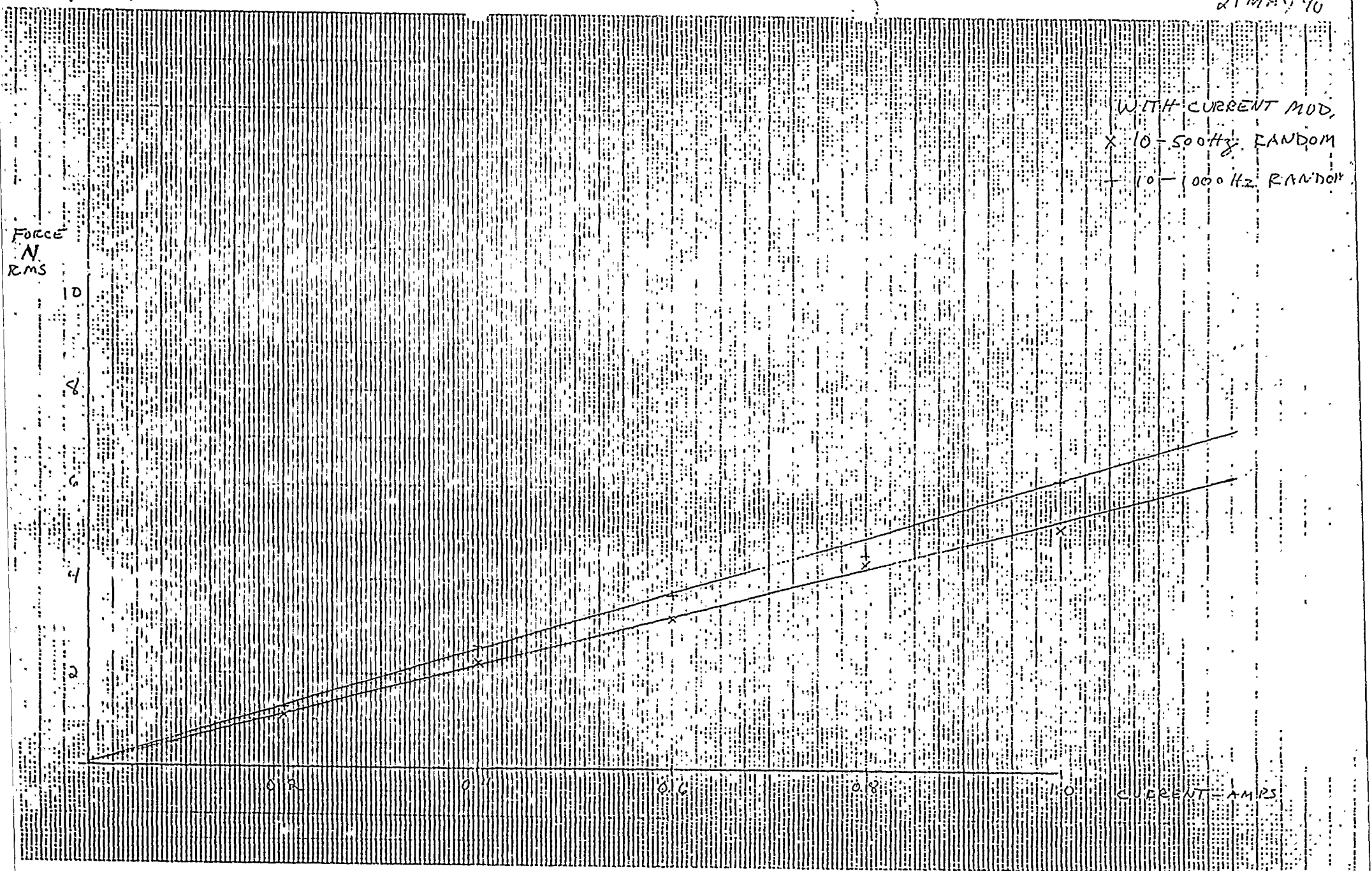

FIGURE 12: COIL CALIBRATION - RANDOM EXCITATION

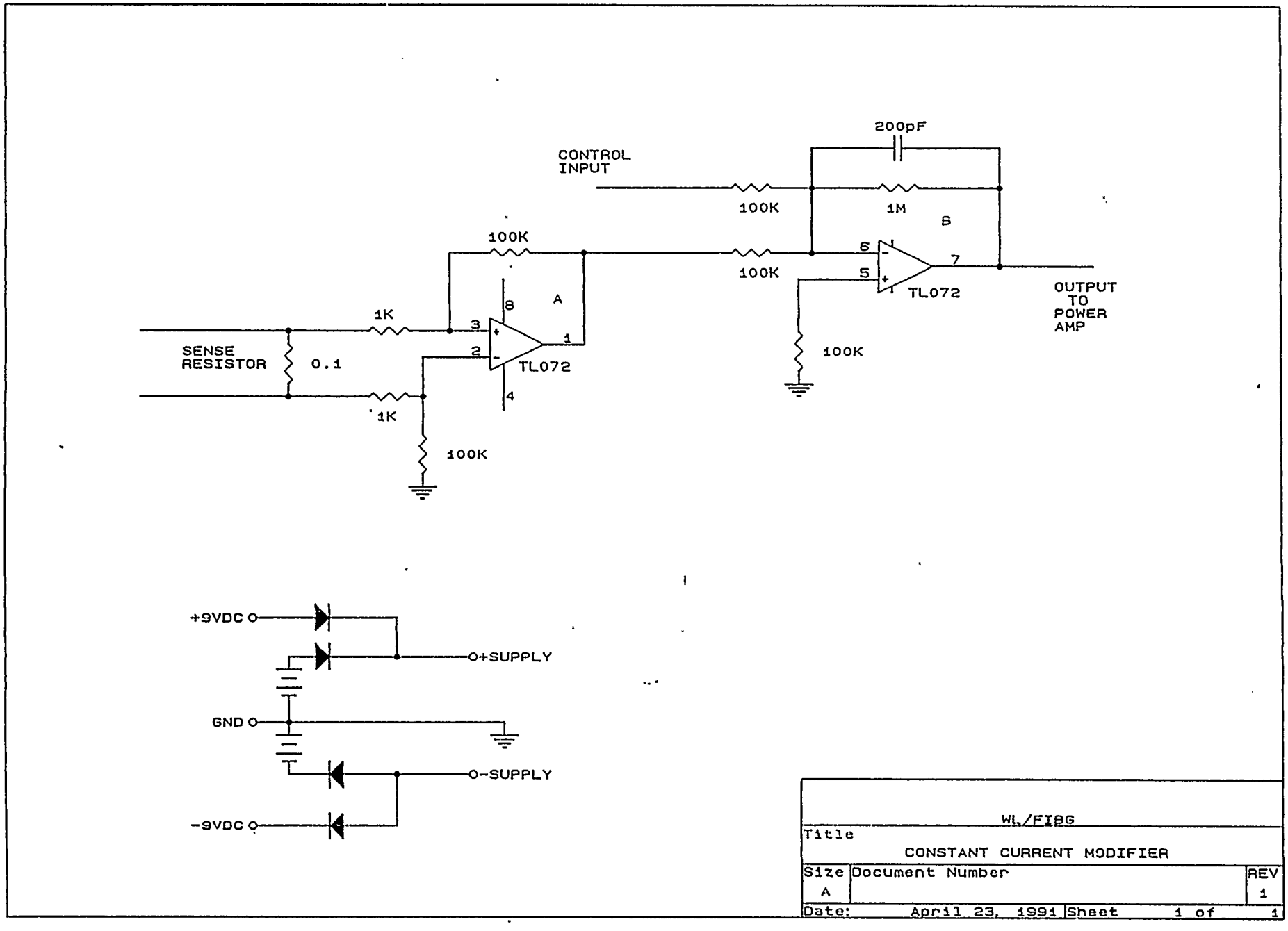

FIGURE 13: CONSTANT CURRENT MODIFIER WIRING ARRANGEMENT AND DESIGN

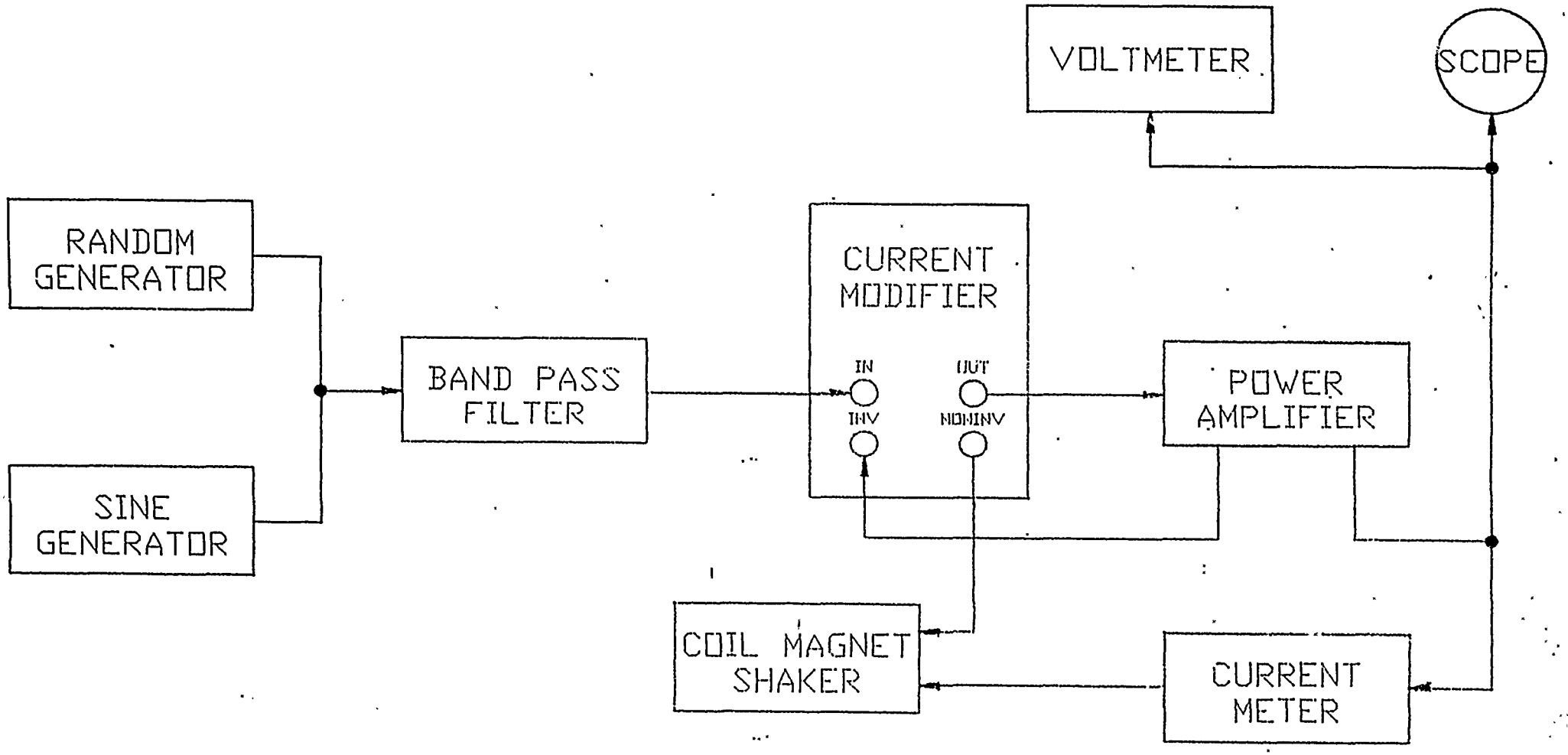

FIGURE 14: TEST SET-UP FOR BEAM EXPERIMENTS

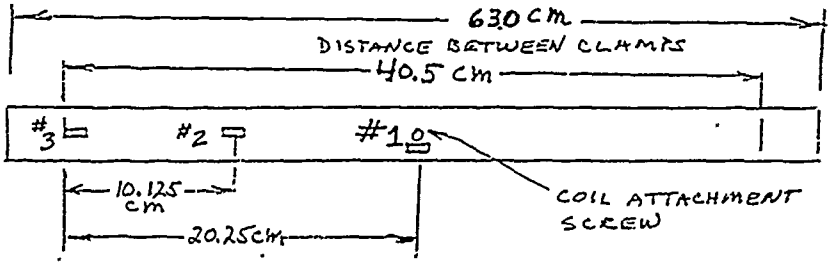

ALUMINUM BEAM STRAIN GAUGE PLAN

SG #4 BACK-TO-BACK WITH #1
SG #5 " " " " #2
SG #6 " " " " #3

FIGURE 15: ALUMINIUM PANEL STRAIN GAUGE PLAN

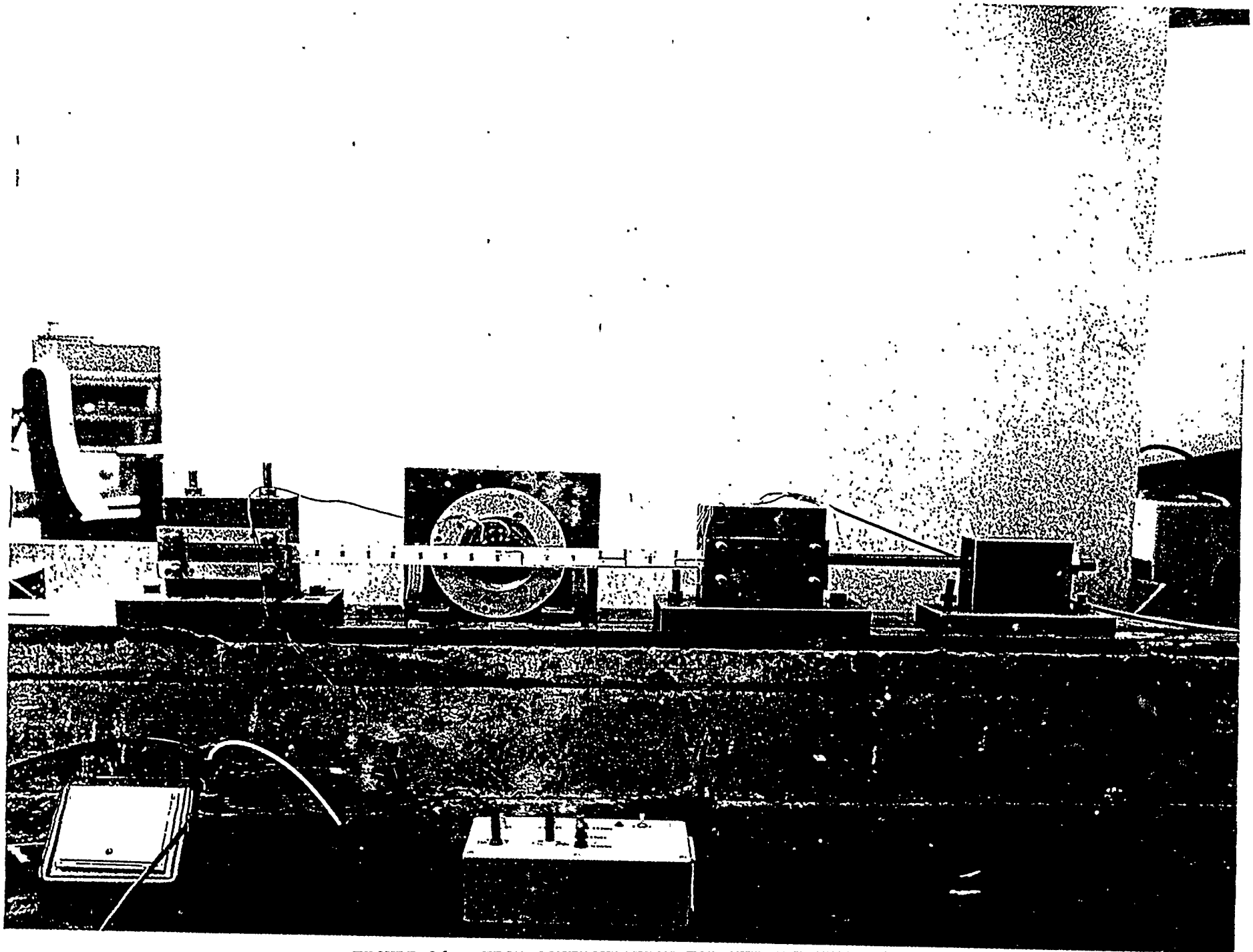

FIGURE 16: TEST CONFIGURATION FOR THE ALUMINIUM C-C BEAM

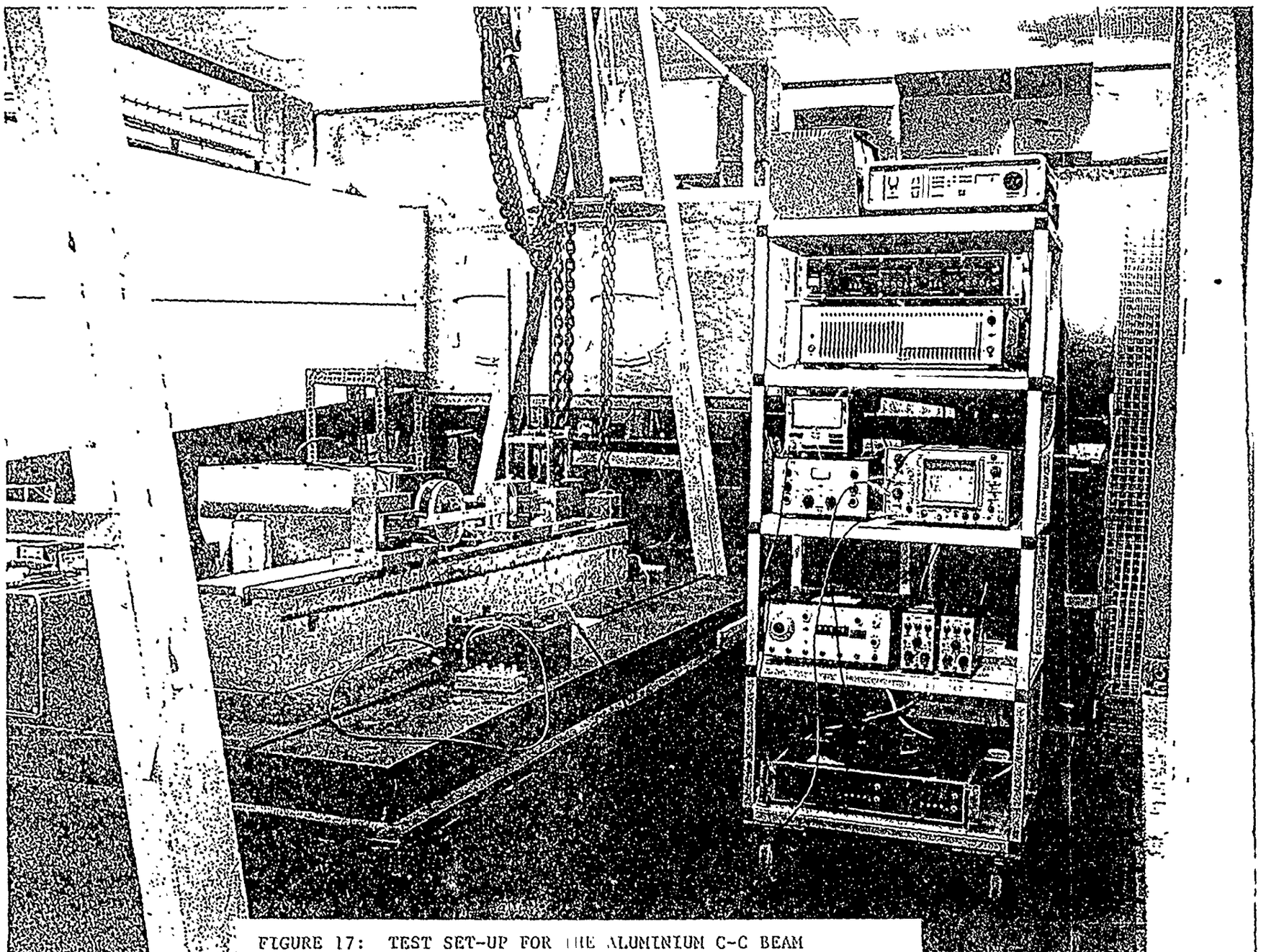

FIGURE 17: TEST SET-UP FOR THE ALUMINIUM C-C BEAM

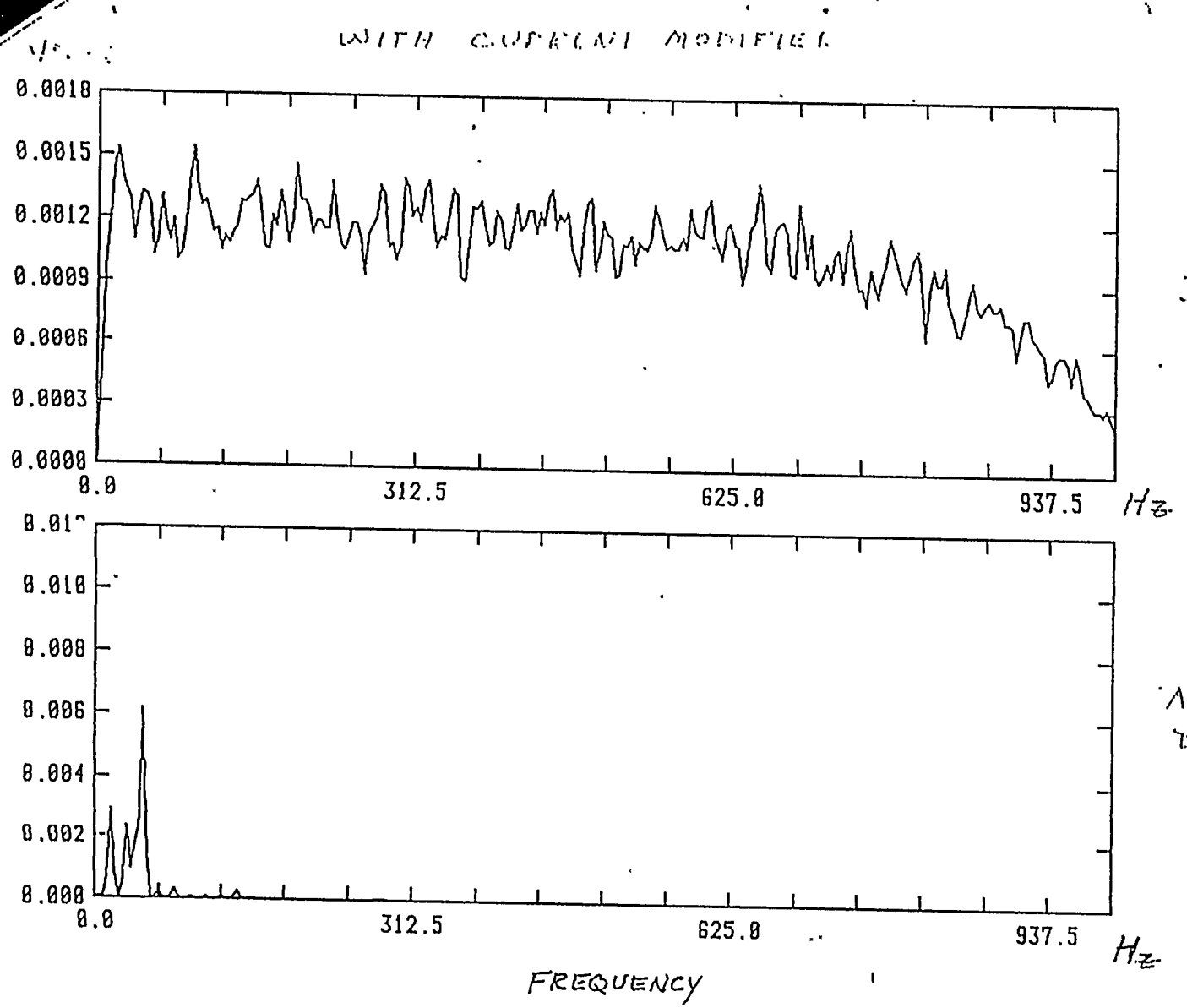

PSD 69 C current
0.25 amps
gain 10

COIL
INPUT
0.25 AMPS

PSD 69 AD
gain 1000

ACCELEROMETER
DISPLACEMENT

FIGURE 18: PSD INPUT AND OUTPUT (DISPLACEMENT) FOR 0.25 AMPS WITH CURRENT MODIFIER

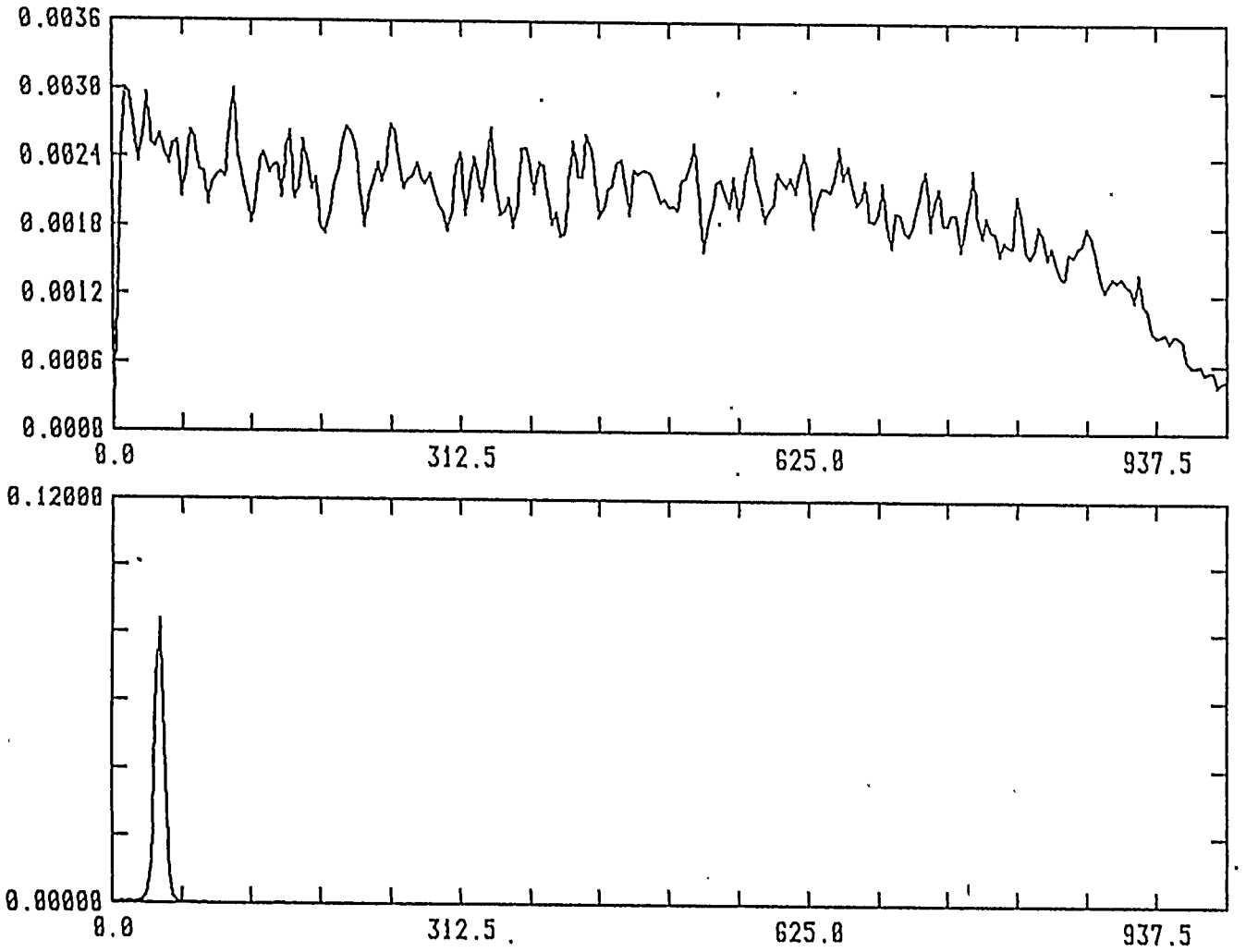

PSD 70 C
0.35 amps
gain 10

0.35 AMPS

PSD 70 AD
gain 1000

ACCELEROMETER
DISPLACEMENT

FIGURE 19: PSD INPUT AND OUTPUT (DISPLACEMENT) FOR 0.35 AMPS WITH CURRENT MODIFIER

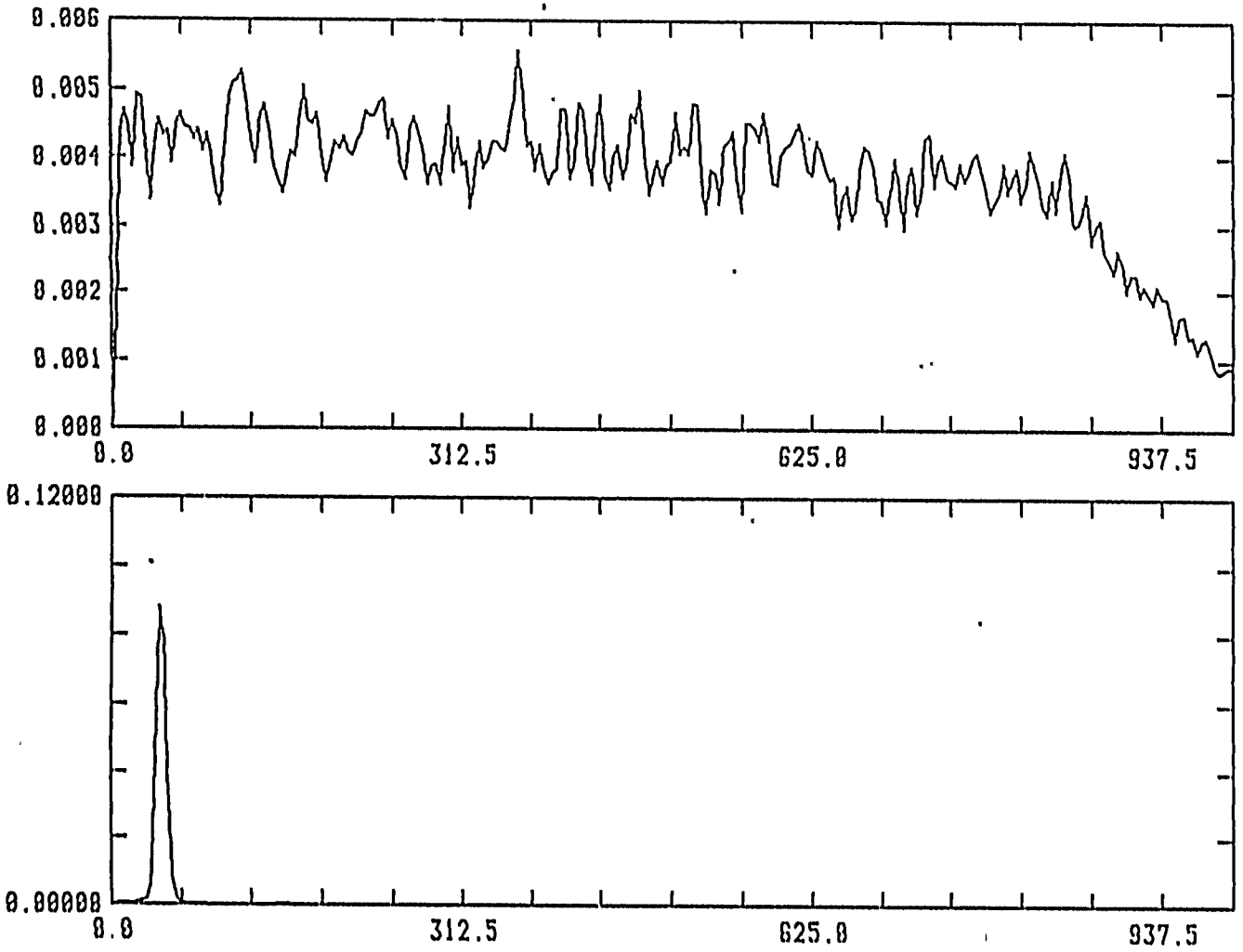

0.5 AMPS

PSD 71C
0.5 amps
Gain 10

PSD 71AD
gain 31.6 x10

ACCELEROMETER
DISPLACEMENT

FIGURE 20: PSD INPUT AND OUTPUT (DISPLACEMENT) FOR 0.5 AMPS WITH CURRENT MODIFIER

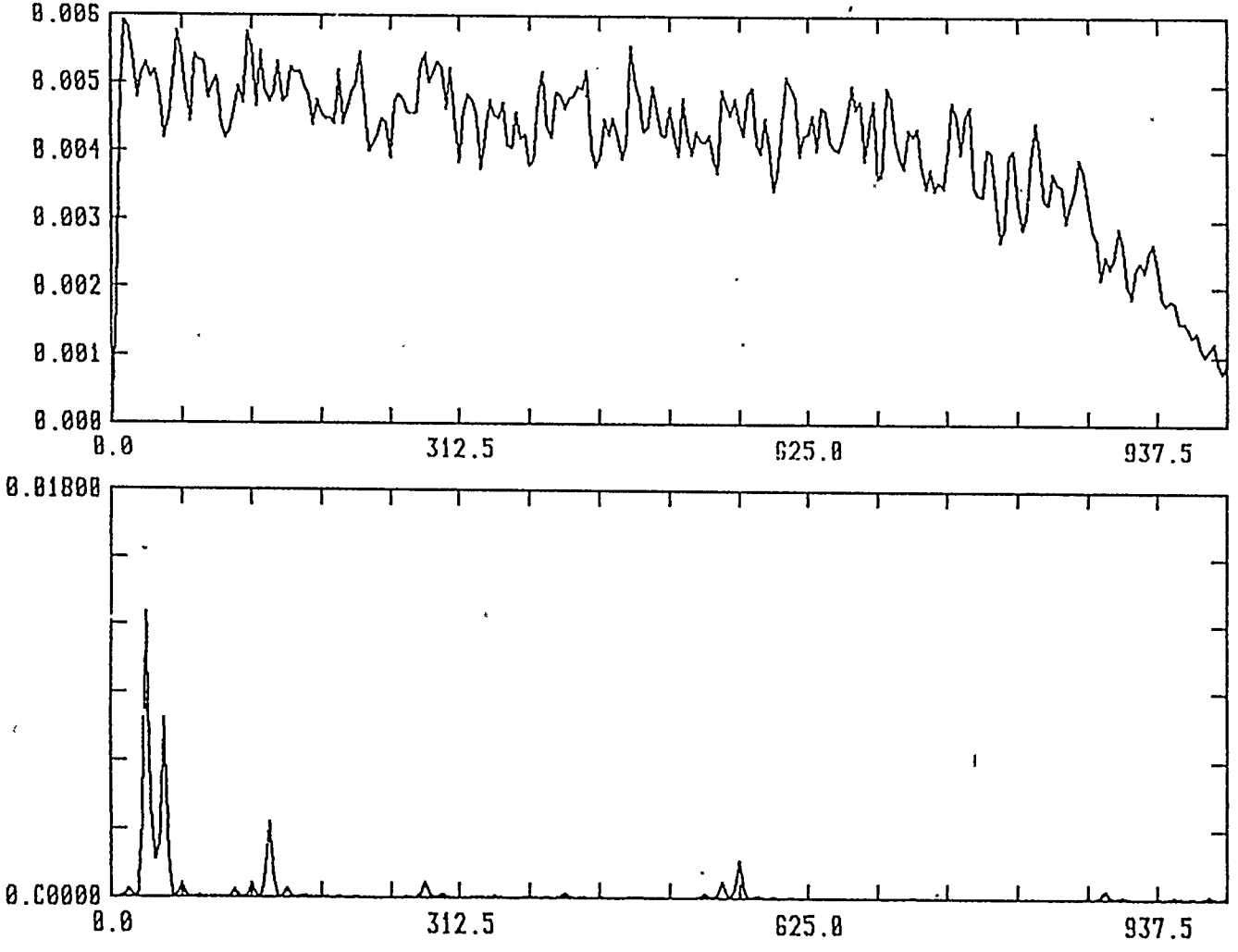

PSD 72 C

0.5 AMPS

PSD 72 A Vel

gain
31.6 X 10

ACCELEROMETER

VELOCITY

FIGURE 21: PSD INPUT AND OUTPUT (VELOCITY) FOR 0.50 AMPS WITH CURRENT MODIFIER

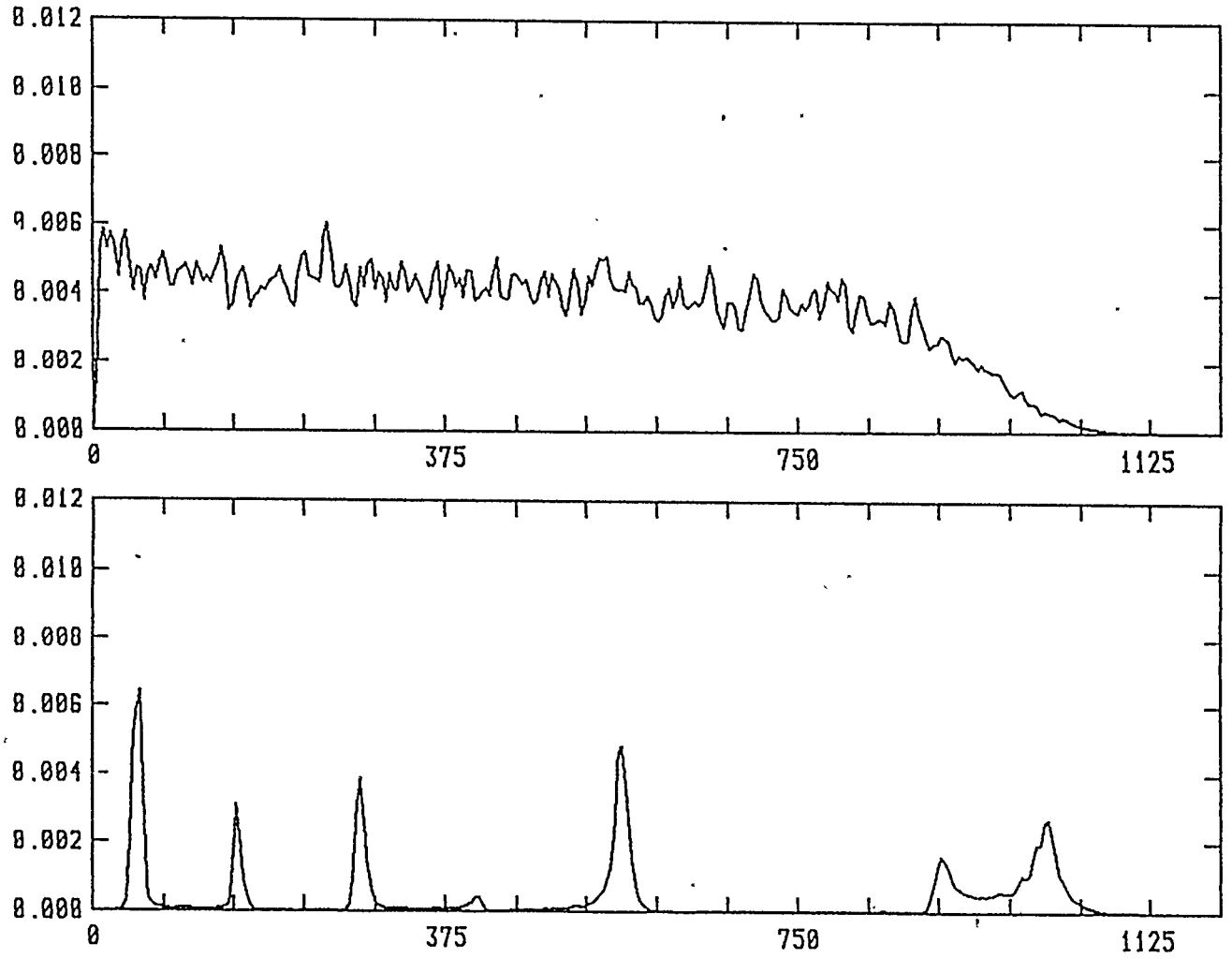

PSD 73C
gain X10

0.5 AMPS

PSD 73A Accel
gain 31.6

ACCELEROMETER
ACCELERATION

FIGURE 22: PSD INPUT AND OUTPUT (ACCELERATION) FOR 0.50 AMPS WITH CURRENT MODIFIER

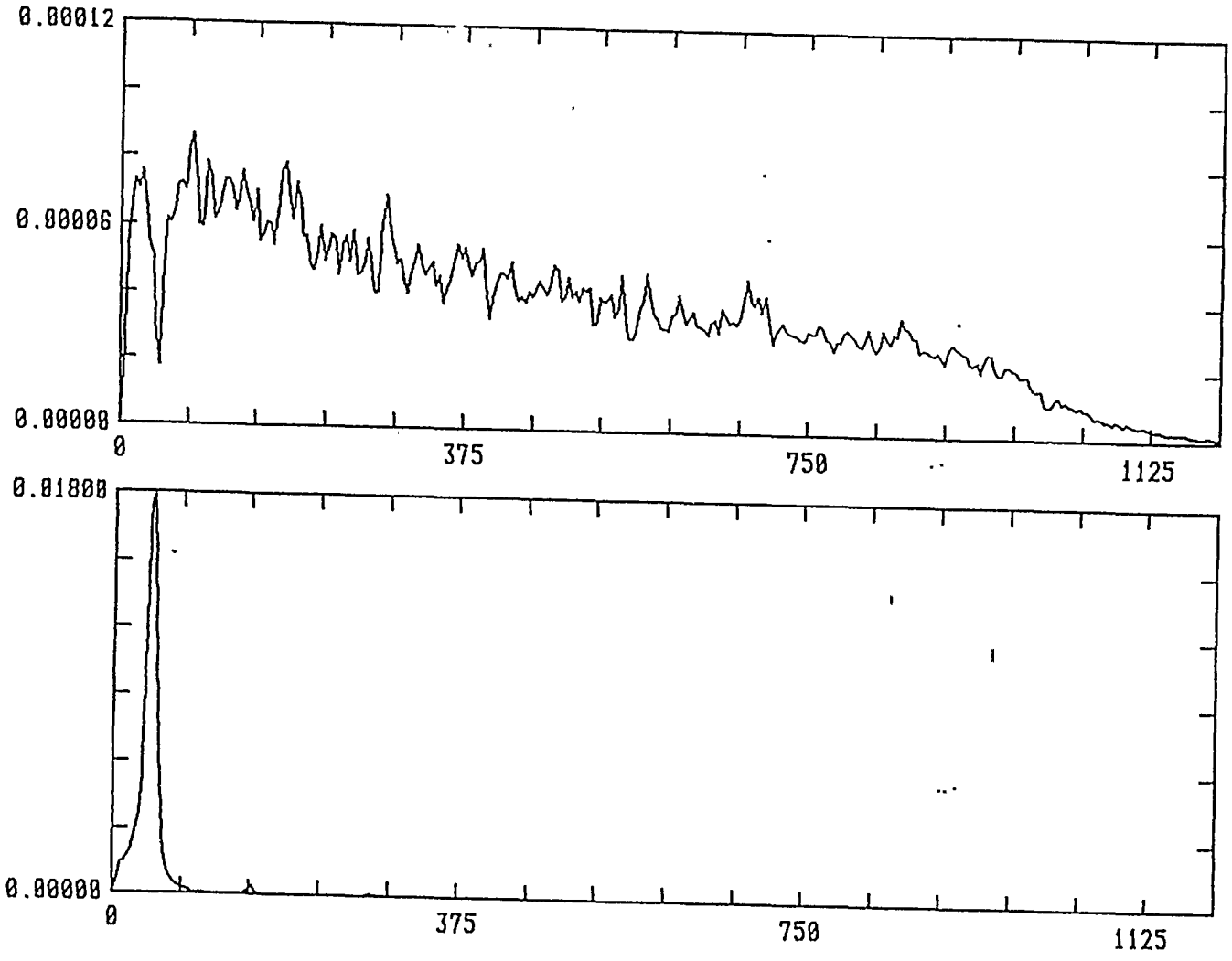

INPUT WITHOUT CURRENT MODIFIER 0.4 AMP

PSD 7.4, C 0.4A
gain X10
W/O CUR MOD

PSD 7.4.1 D

ACCELEROMETER DISPLACEMENT

FIGURE 23: PSD INPUT AND OUTPUT (DISPLACEMENT) FOR 0.4 AMPS WITHOUT CURRENT MODIFIER

same gain as 74

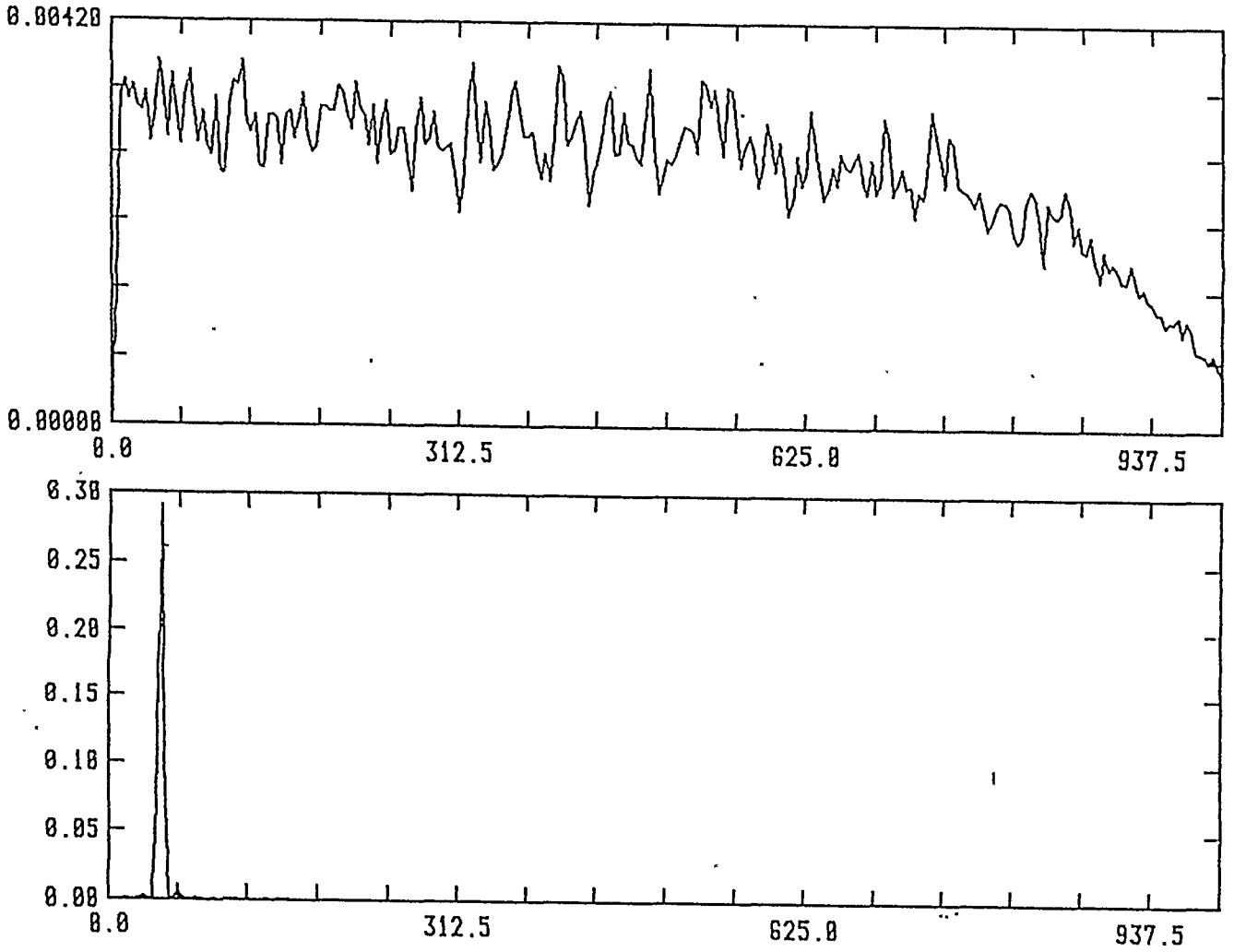

PSD 75C

INPUT WITH CURRENT MODIFIER 0.4 AMPS

ACCELEROMETER DISPLACEMENT PSD 754D

FIGURE 24: PSD INPUT AND OUTPUT (DISPLACEMENT) FOR 0.4 AMPS WITH CURRENT MODIFIER

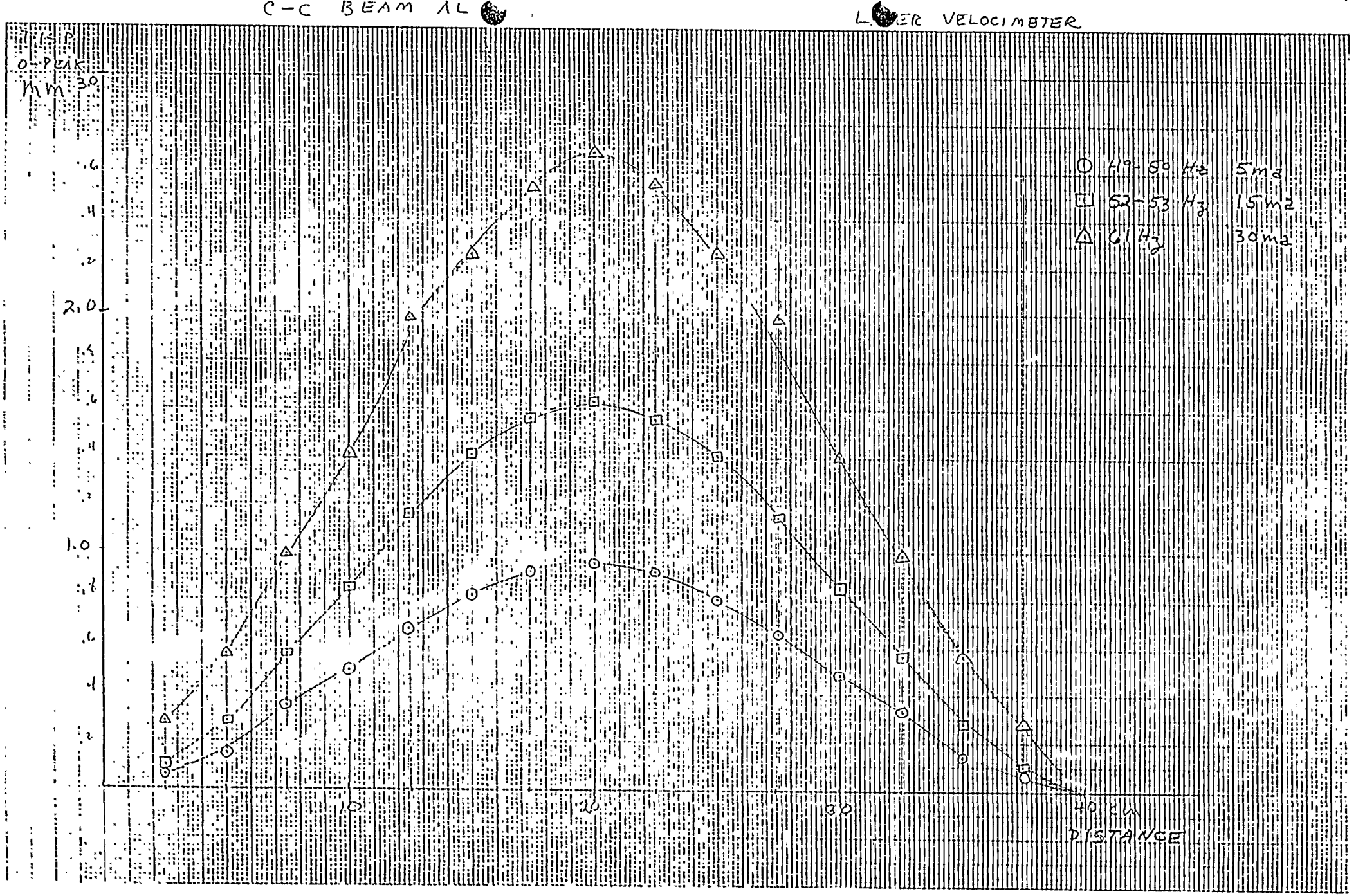

FIGURE 25: DISPLACEMENT MEASUREMENTS C-C BEAM

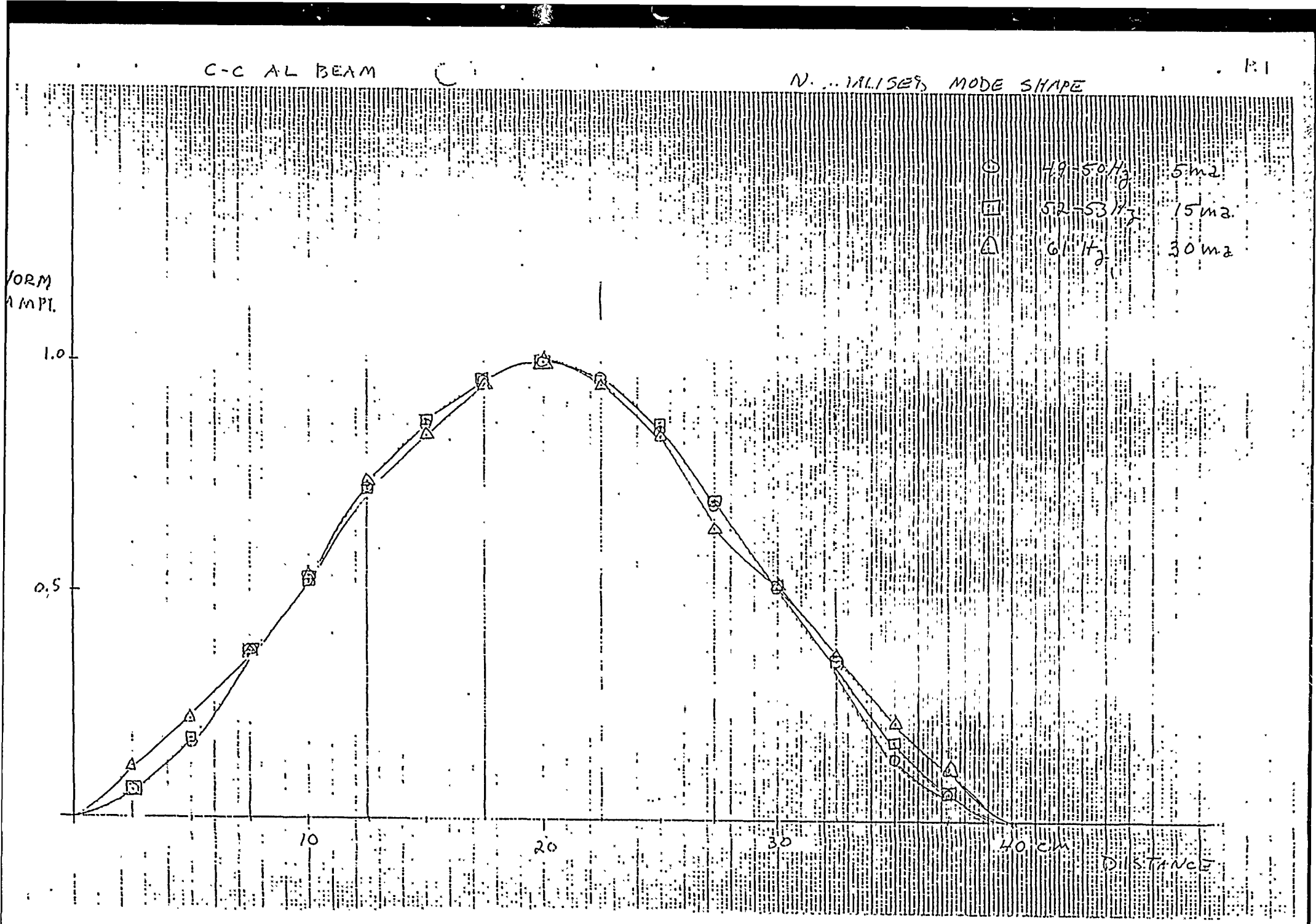

FIGURE 26: NORMALISED DISPLACEMENT MEASUREMENTS

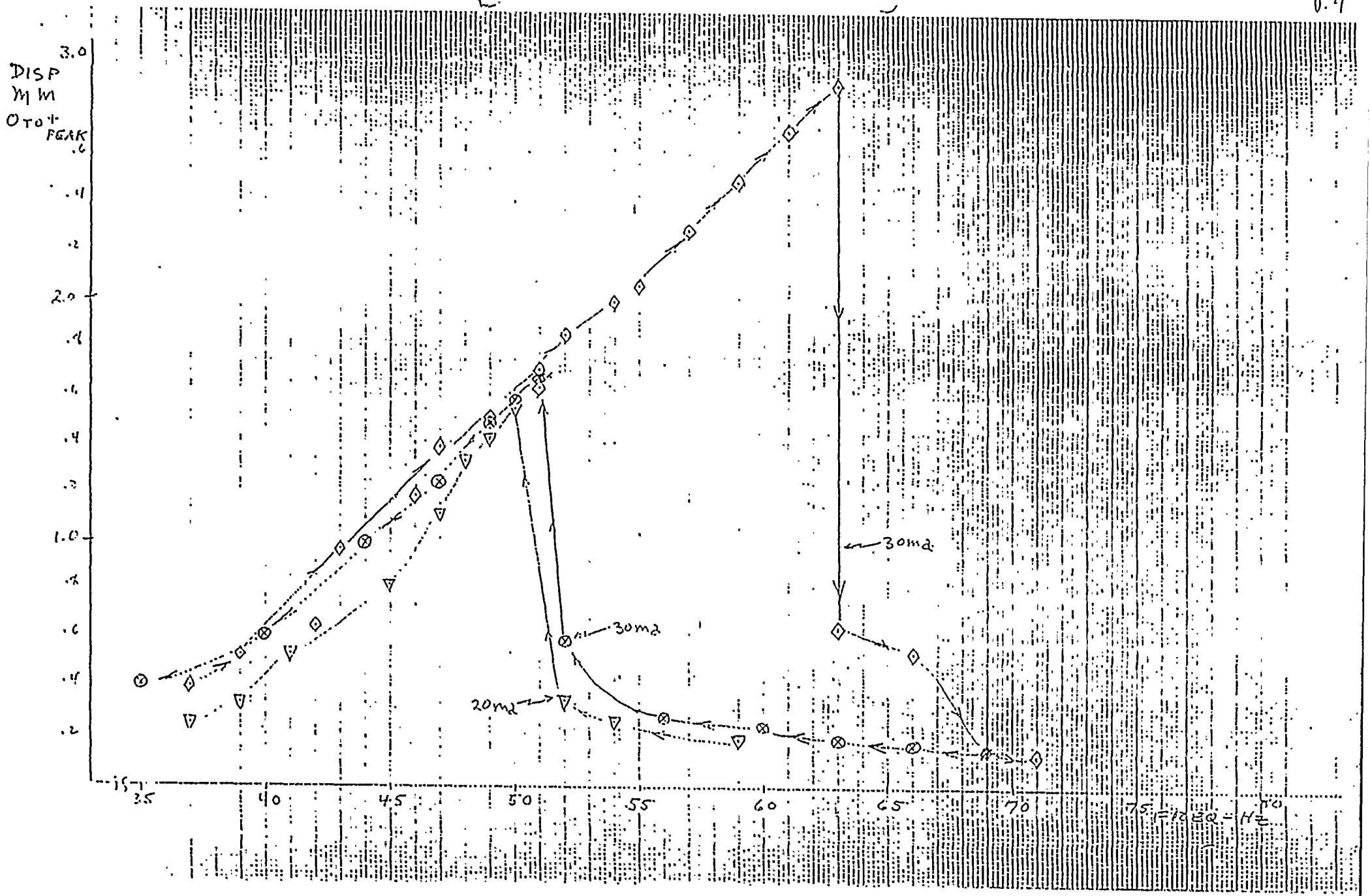

FIGURE 27: SLOW SINE SWEEP TEST C-C BEAM

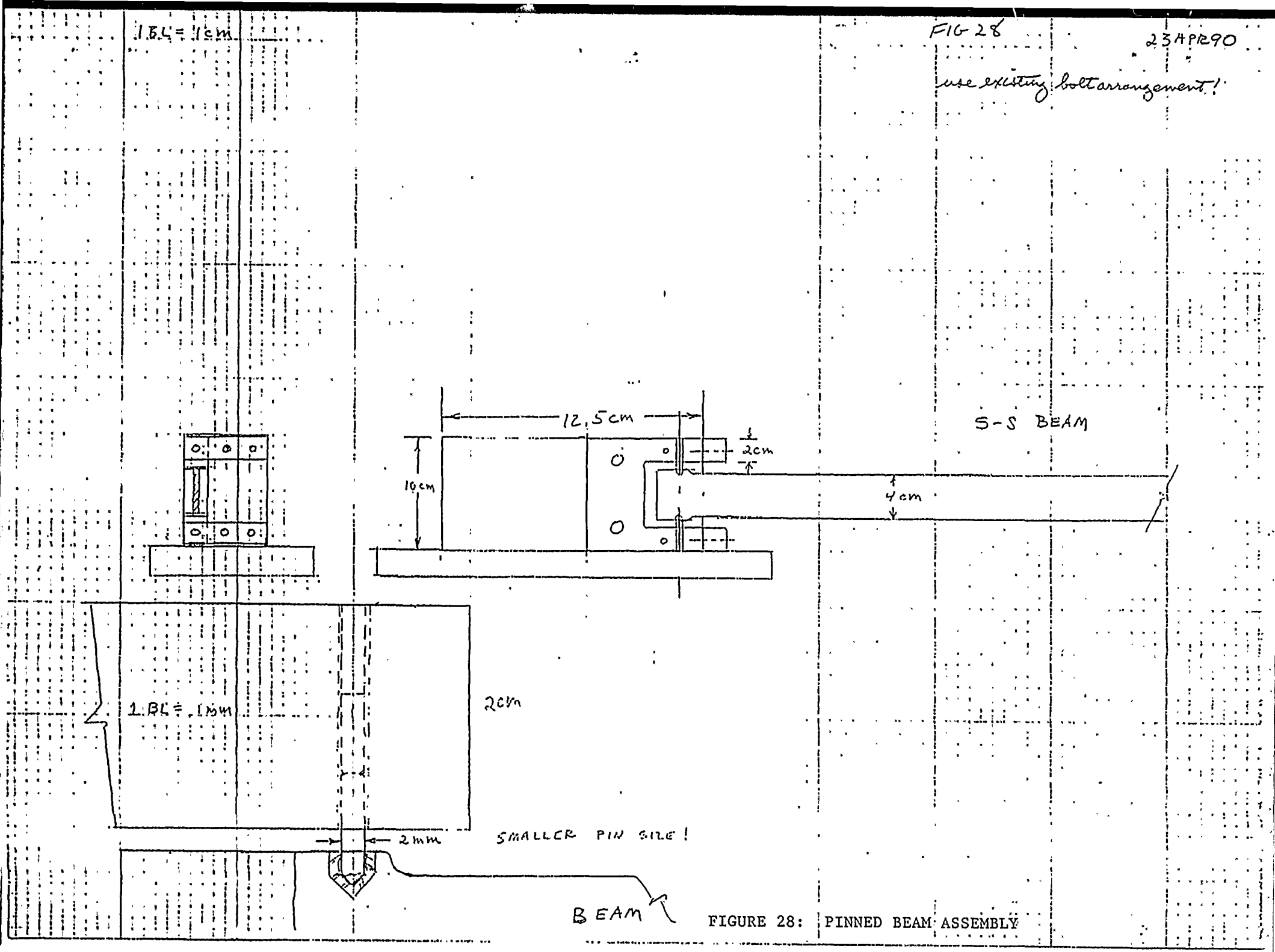

FIGURE 28: PINNED BEAM ASSEMBLY

SCALE 1:1 mm. 7 MAY 90 HEW

ASSEMBLY DRAWING
PINNED BEAM

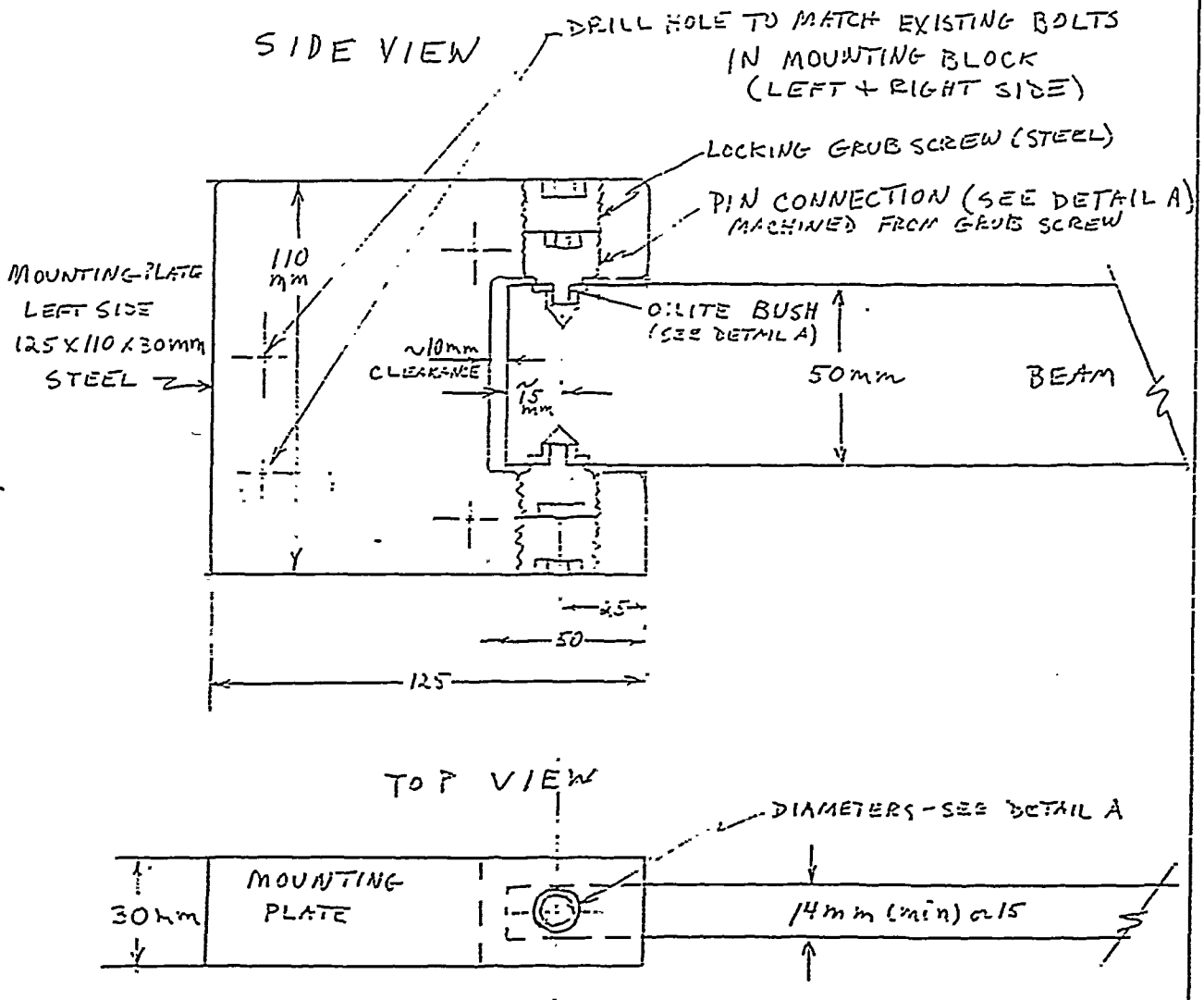

PARTS: 5 ALUMINUM DTD 5070(LOCAL) TEST BEAMS 660 X 50 X ~14 mm (min) ~15mm 1 DRILLED FOR OILITE BUSH
10 OILITE BUSHES
10 MACHINED GRUB SCREWS - STEEL
10 MATCHING LOCKING GRUB SCREWS
2 MOUNTING PLATES - LEFT + RIGHT SIDE - STEEL (125 X 110 X 30 mm)

FIGURE 29: PINNED BEAM ASSEMBLY WITH OILITE BUSH

9MAY90 HJF

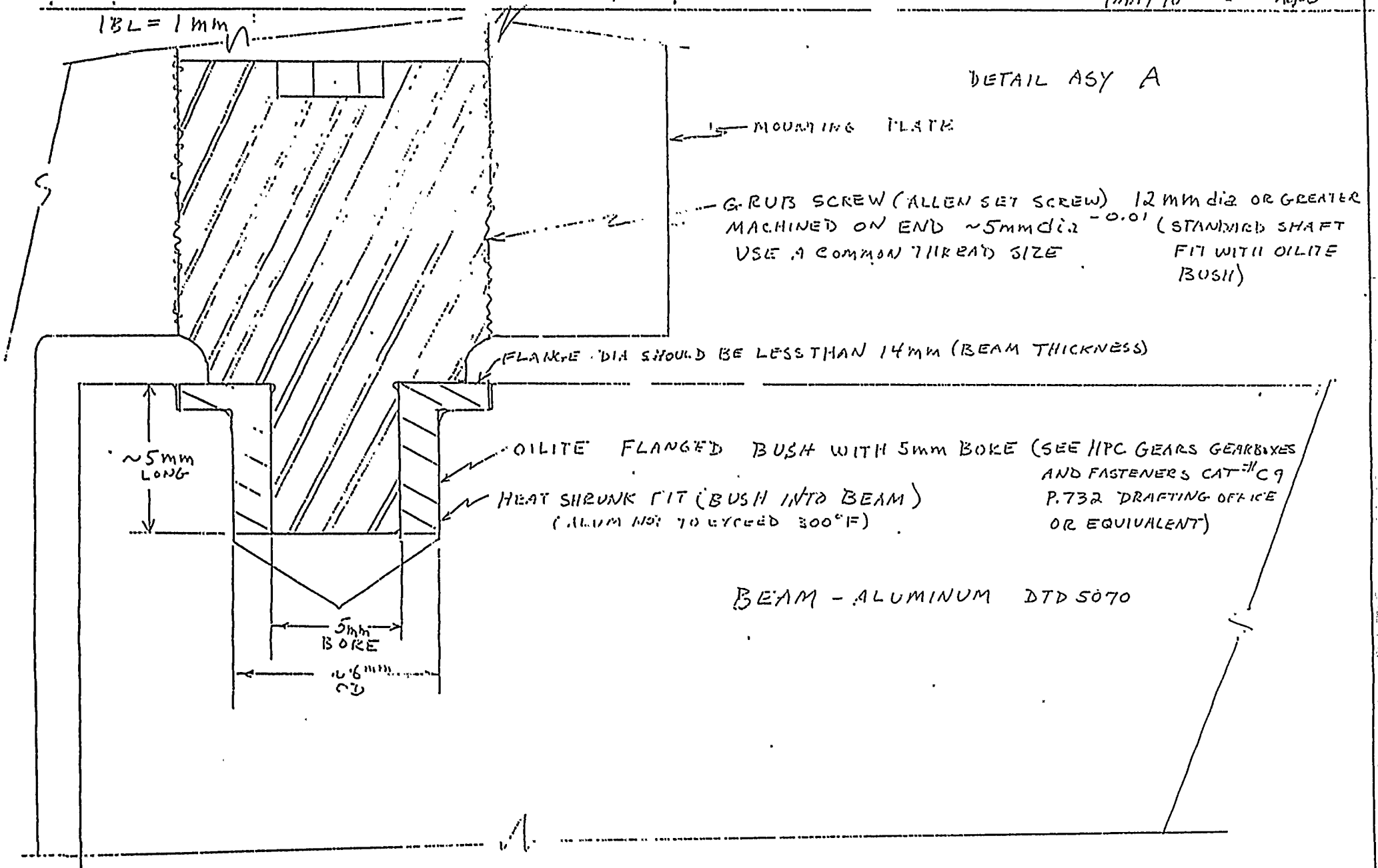

FIGURE 30: DETAIL CONSTRUCTION OF PINNED JOINT

1 BL = 10mm

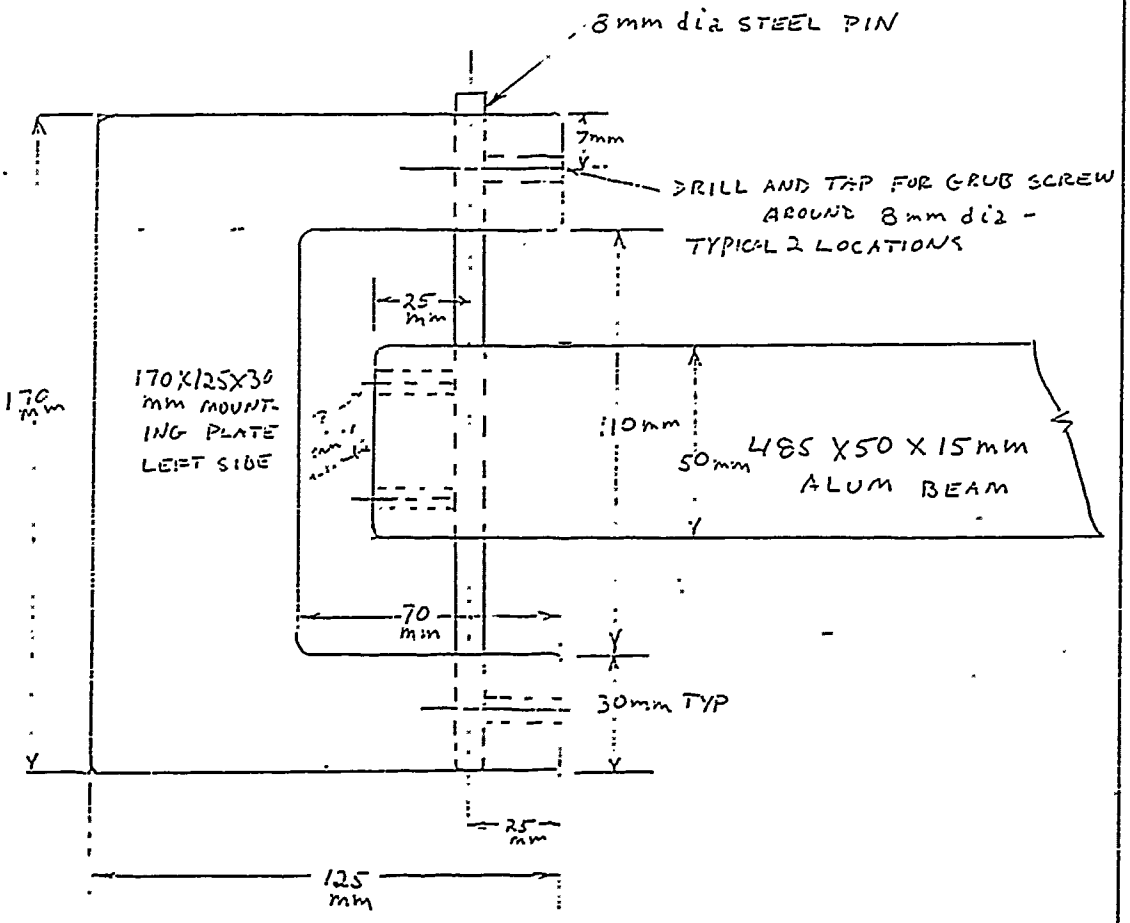

PARTS. 5 ALUMINUM 6TD 5070 (DUREAL) TEST BEAMS 485X50 X ~1/4" min) or 15 (1 DRILLED FOR PIN)
2 STEEL 8mm dia PINS
2 MOUNTING PLATES - LEFT + RIGHT SIDE - STEEL
8 GRUB SCREWS

FIGURE 31: FLEXIBLE END CONSTRAINT BEAM

TIME HISTORY
AFTE. NORMALISING

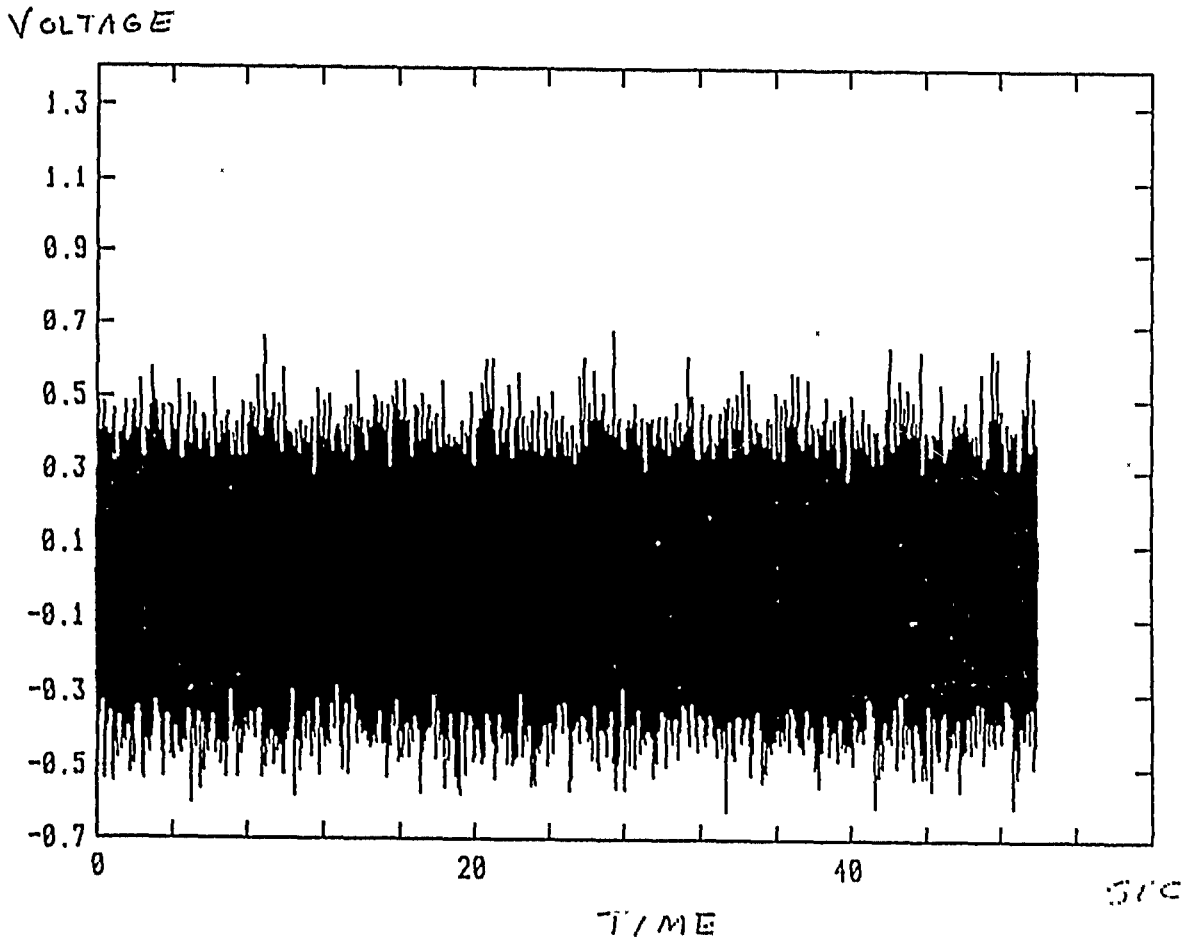

FIGURE 32: EXAMPLE OF RANDOM SIGNALS GENERATED INTERNALLY IN A PC

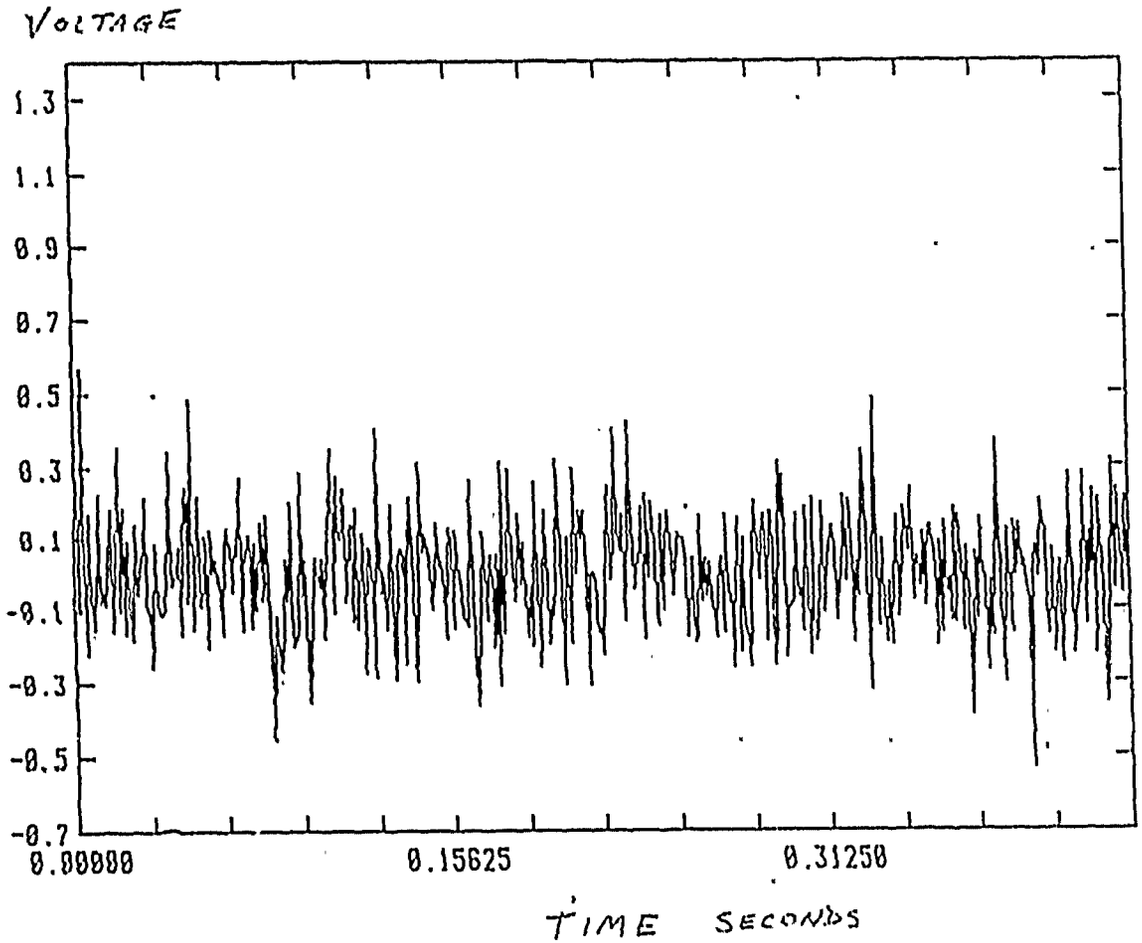

FIGURE 33: EXPANDED TIME HISTORY

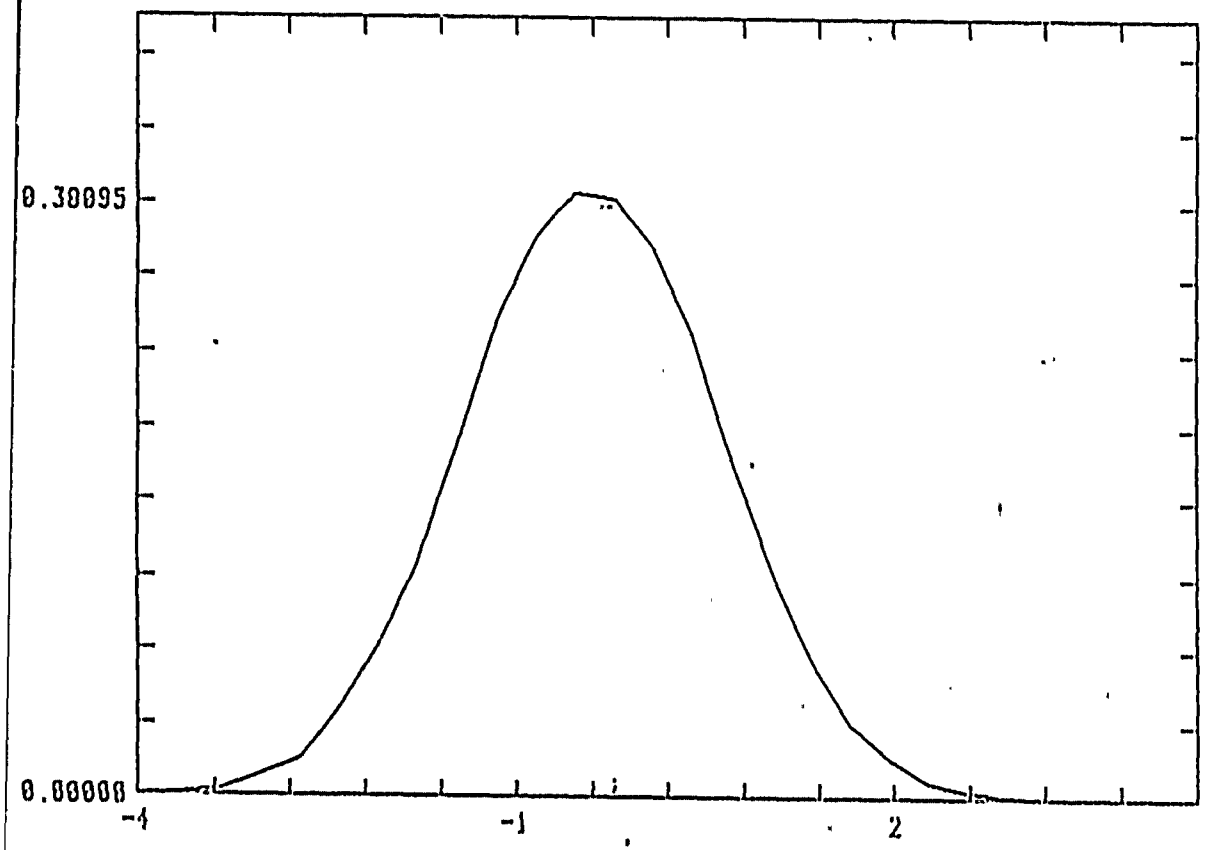

FIGURE 34: PROBABILITY DISTRIBUTION

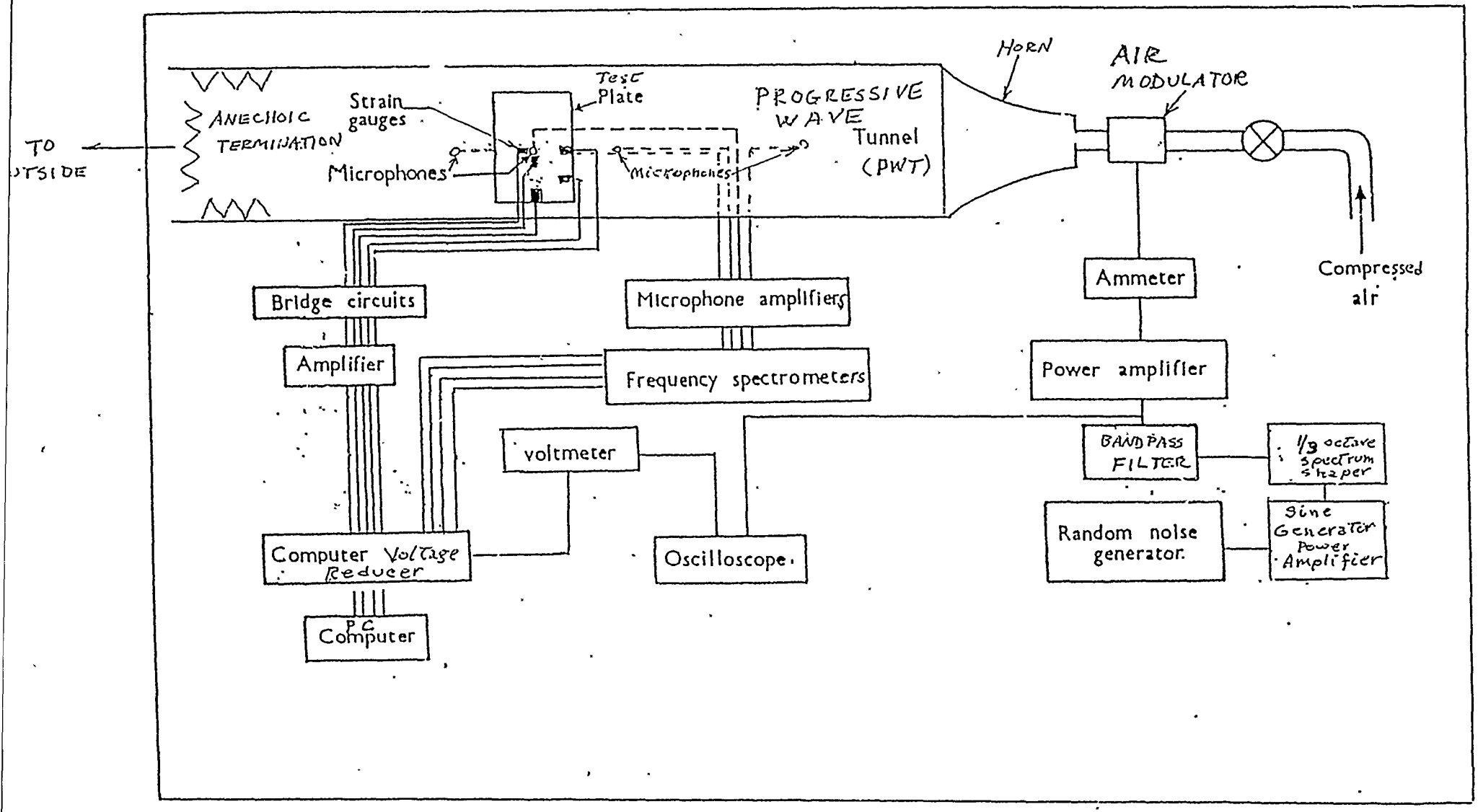

FIGURE 35: INSTRUMENTATION FOR ACOUSTIC TESTS

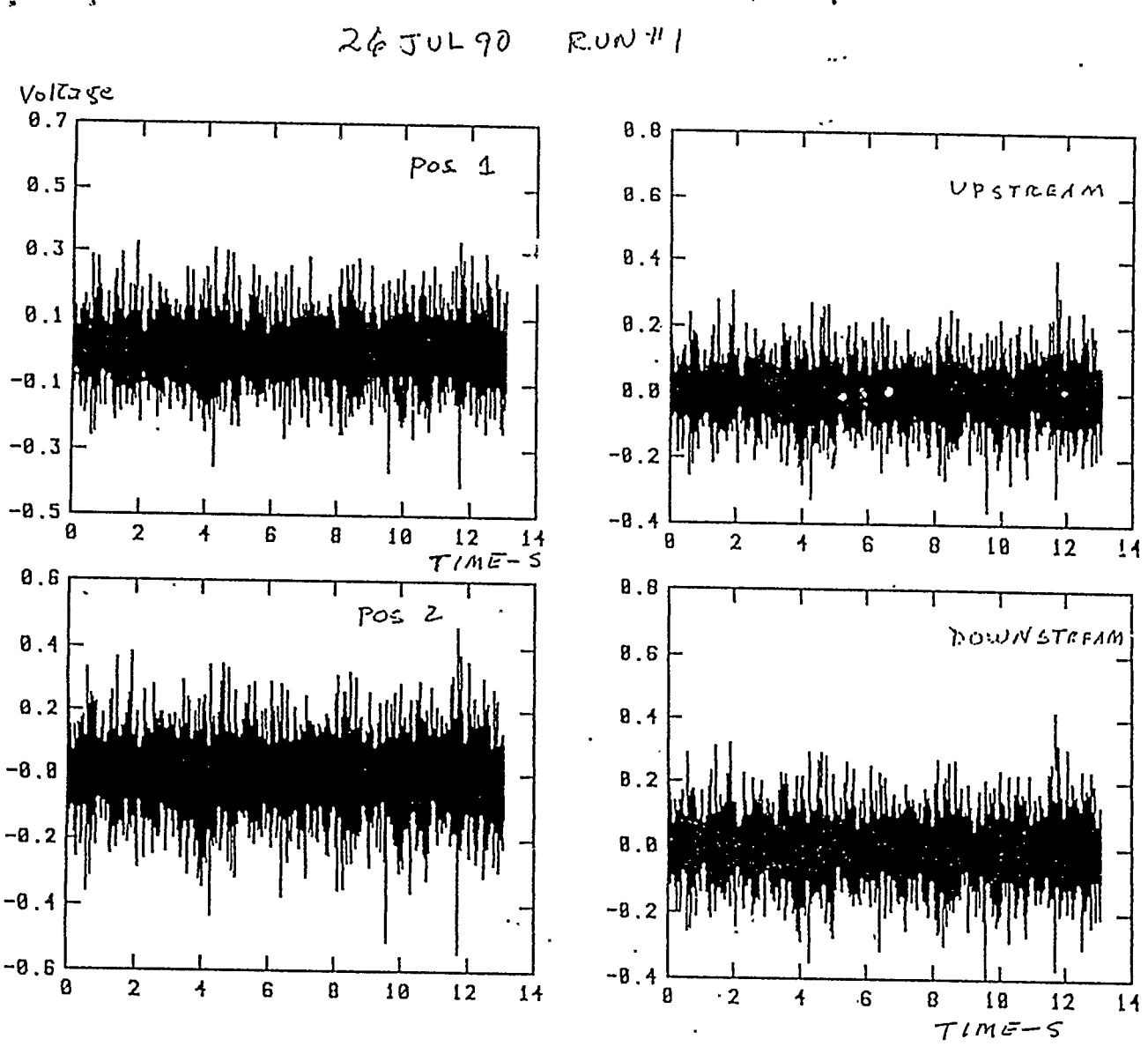

FIGURE 36: MICROPHONE TIME HISTORIES AT FOUR LOCATIONS

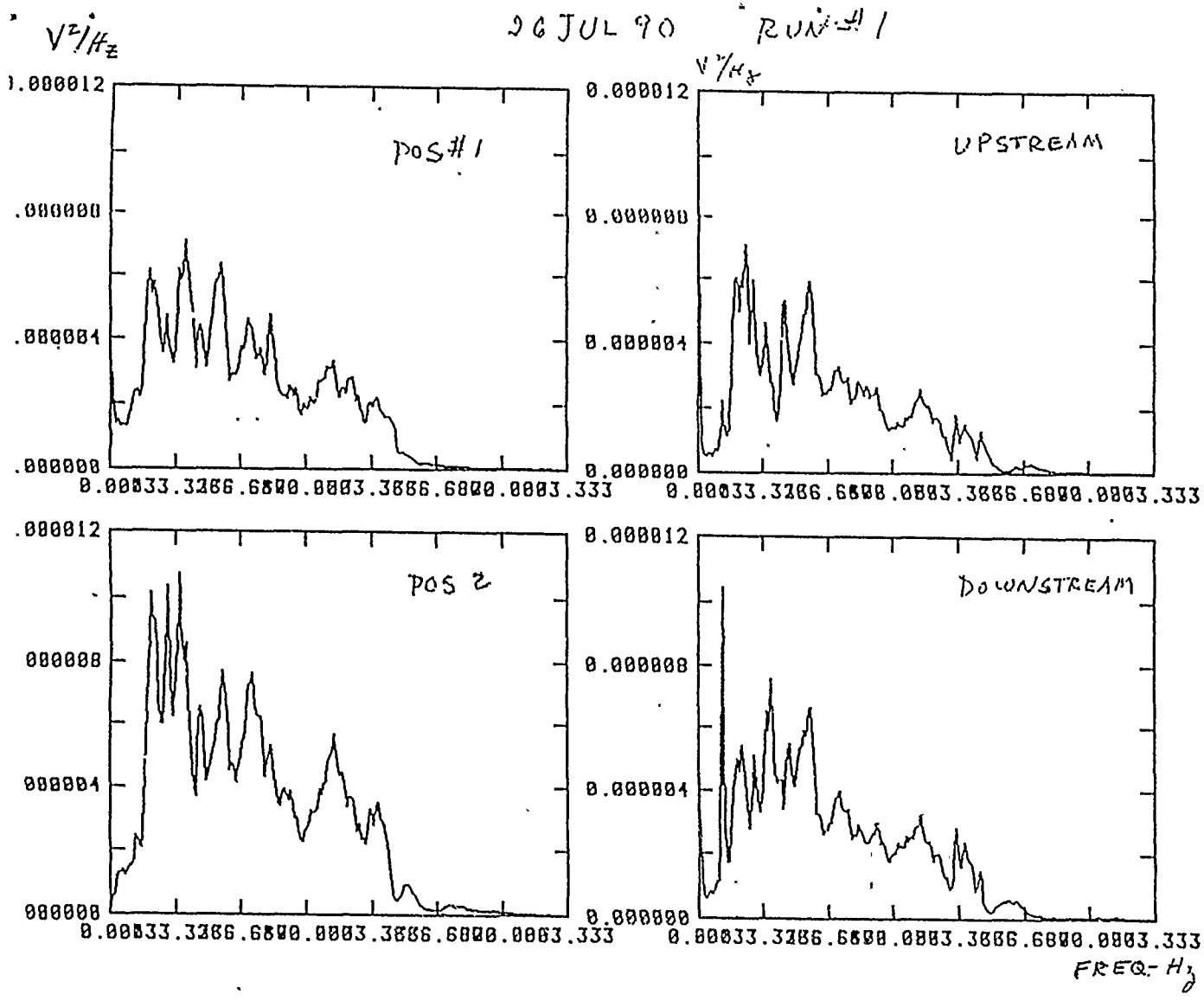

FIGURE 37: MICROPHONE PSD'S AT FOUR LOCATIONS

FREQ.DAC

10132PSD.D@0133PSD.DAC

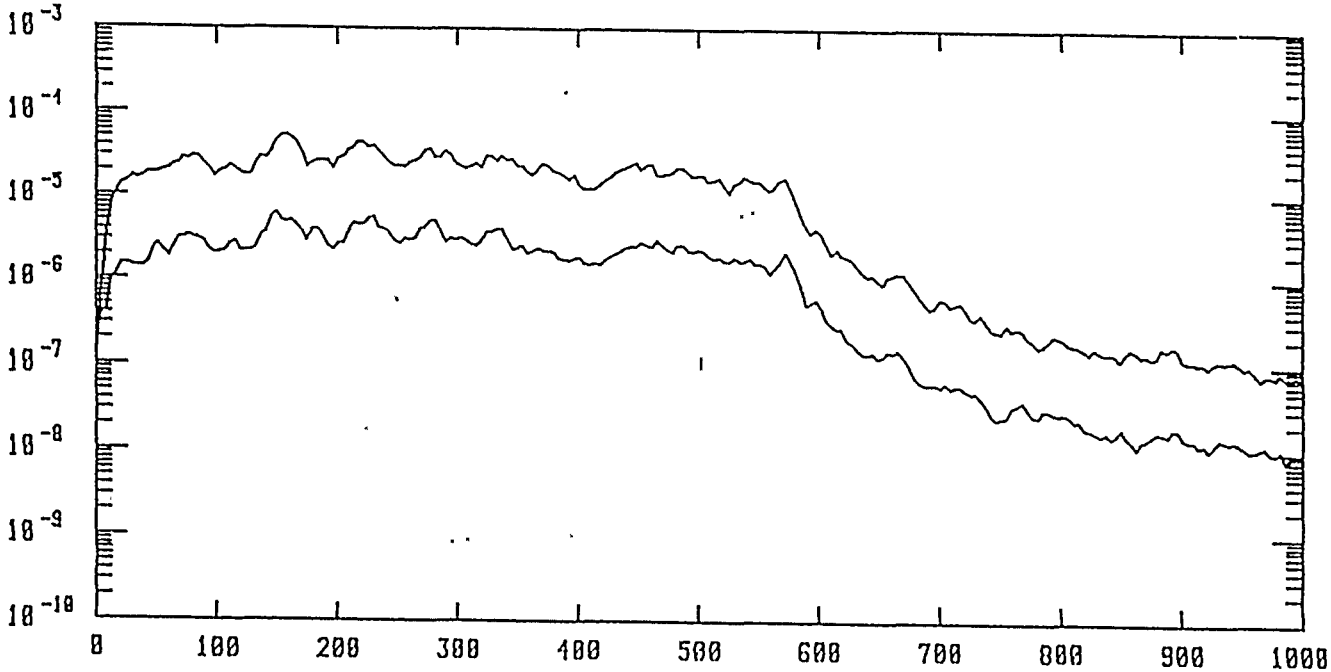

FIGURE 38: COMPARISON OF TWO LEVELS, MIC #1

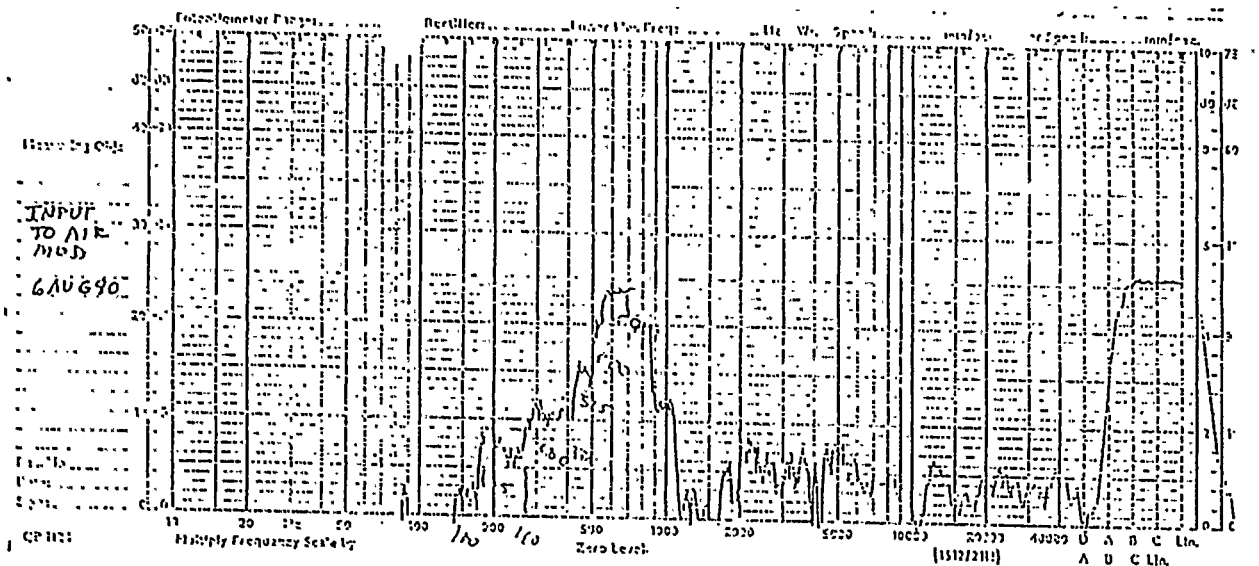

FIG INPUT SPECTRUM TO AIR MODULATOR

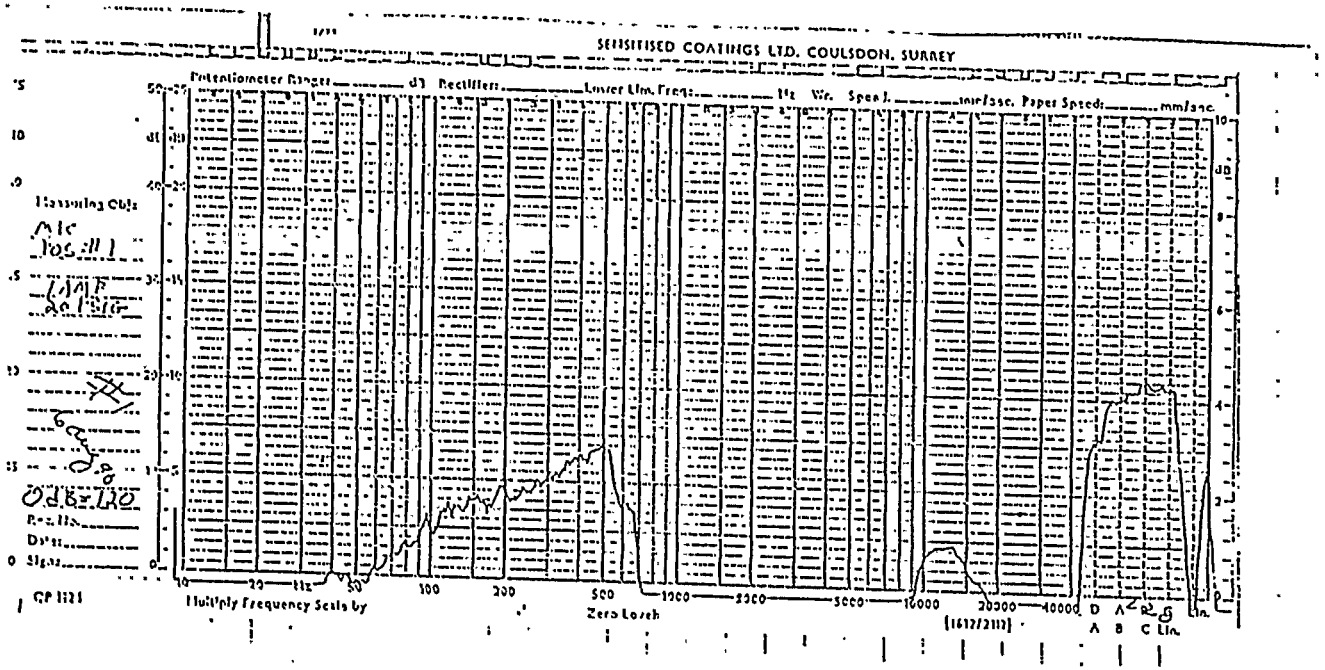

FIGURE 39: 1/3 OCT SPECTRUM OF MIC #1 IN PWT

2 JUL 90

ALUM PANEL SG PLAN

1BL = 2 cm

10 GAUGES
5 BACK TO BACK

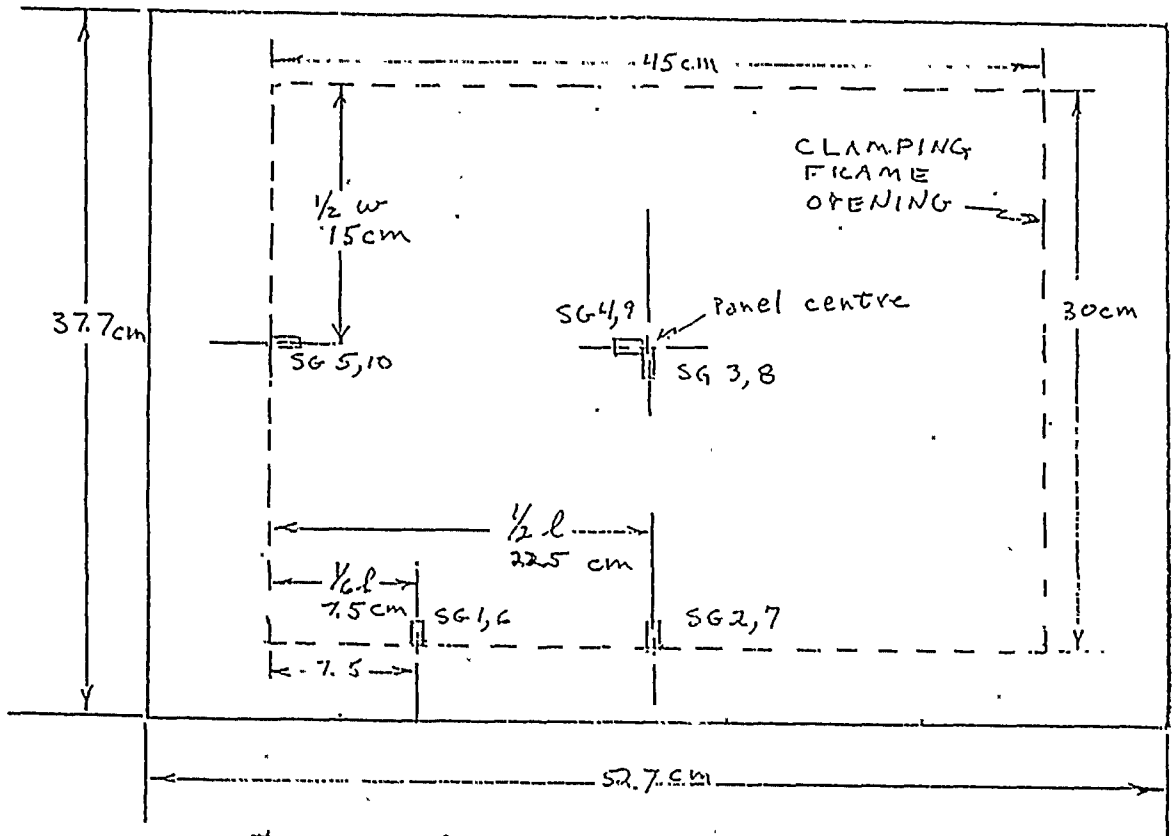

SG # 1, 2, 3, 4, 5 → INSIDE DUCT
SG # 6, 7, 8, 9, 10 → OUTSIDE DUCT
} STRAIN GAUGE PAIRS ARE BACK TO BACK

l = LENGTH
w = WIDTH

FIGURE 40: STRAIN GAUGE PLAN ALUMINIUM PLATE

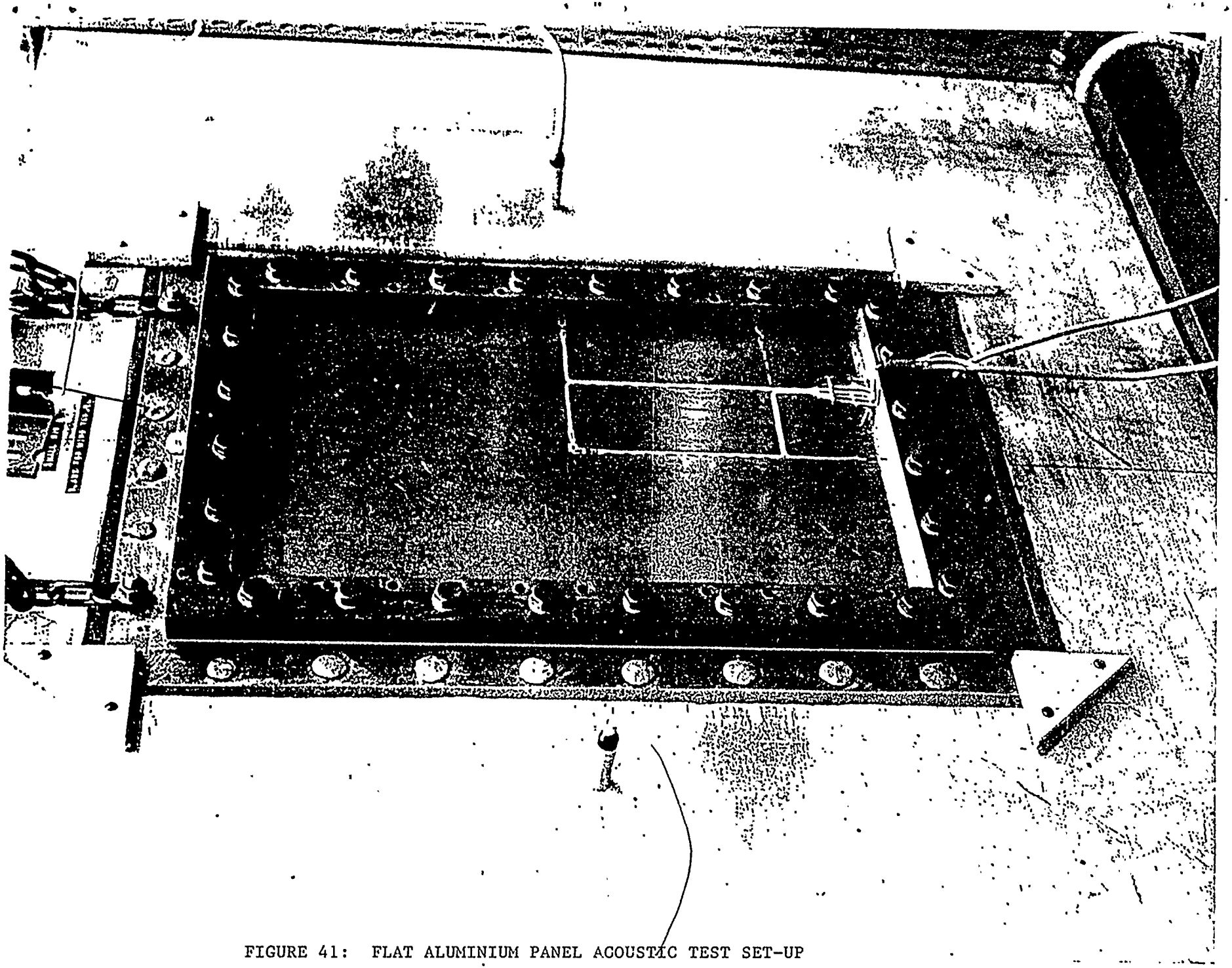

FIGURE 41: FLAT ALUMINIUM PANEL ACOUSTIC TEST SET-UP

SG#1

E\DATA\10312.DAT channel 2 :6AUG90 ACOUS TEST 1AMP 140dB

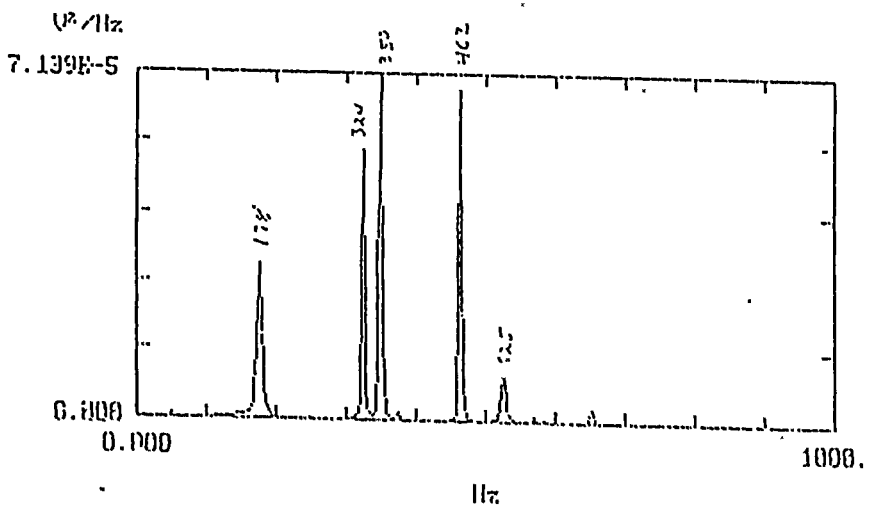

SG#2

D:WOLFE\DATA\10316.DAT channel 2 :6AUG90 ACOUS TEST

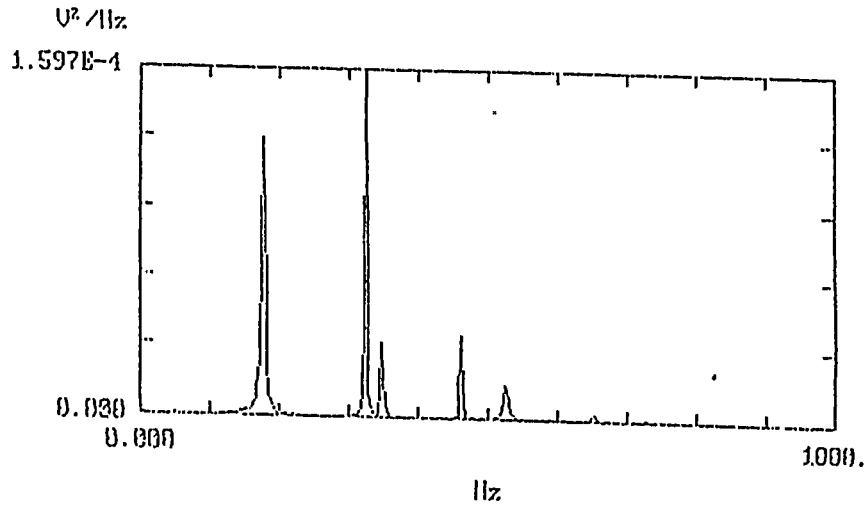

SG#6

LFE\DATA\10314.DAT channel 3 :6AUG90 ACOUS TEST 1AMP

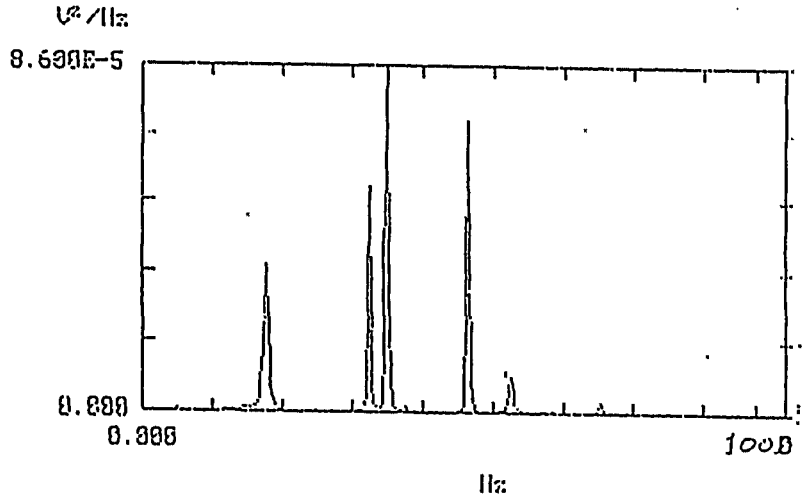

SG#7

D:WOLFE\DATA\10310.DAT channel 3 :6AUG90 ACOUS TEST

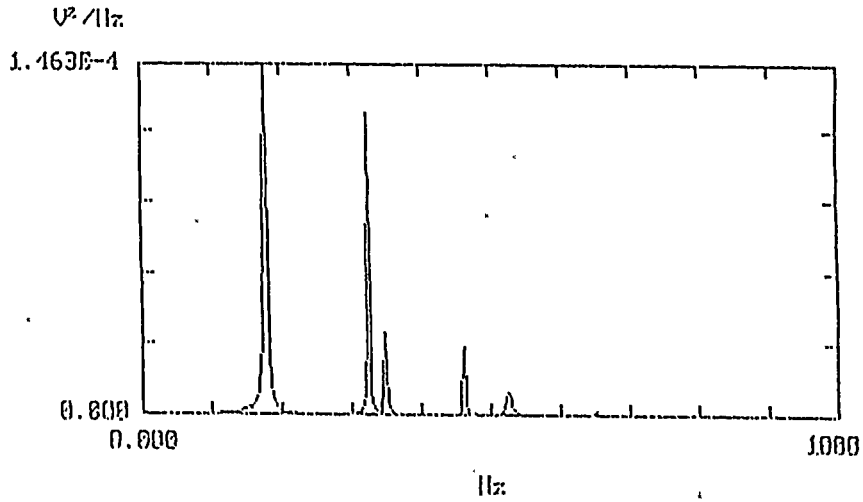

FIGURE 42: PSD STRAIN GUAUGE PAIRS 1 & 6 and 2 & 7 140 dB O/A

SG#1 1.5 amp

\DATA\10421.DAT channel 2 :10AUG90 ACOUS TEST 146DB (TOTAL)

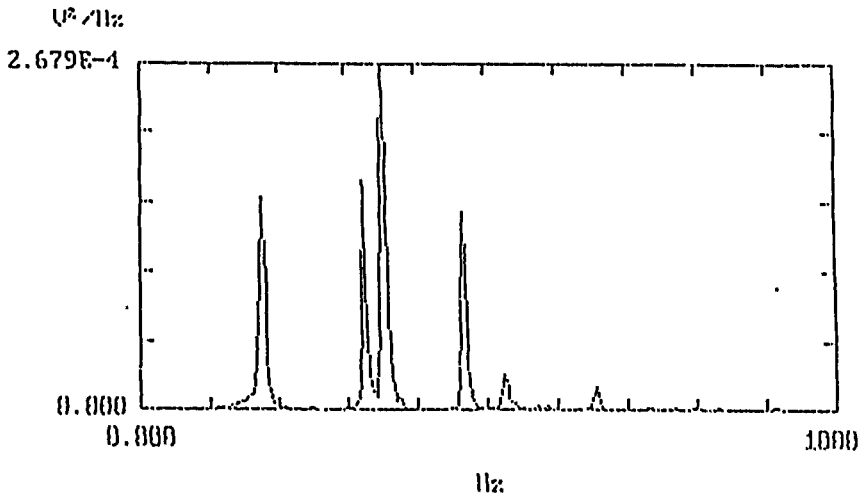

SG#6 1.5 amp 146.5dB

E\DATA\10401.DAT channel 3 :10AUG90 ACOUS TEST 146DB (TOTAL)

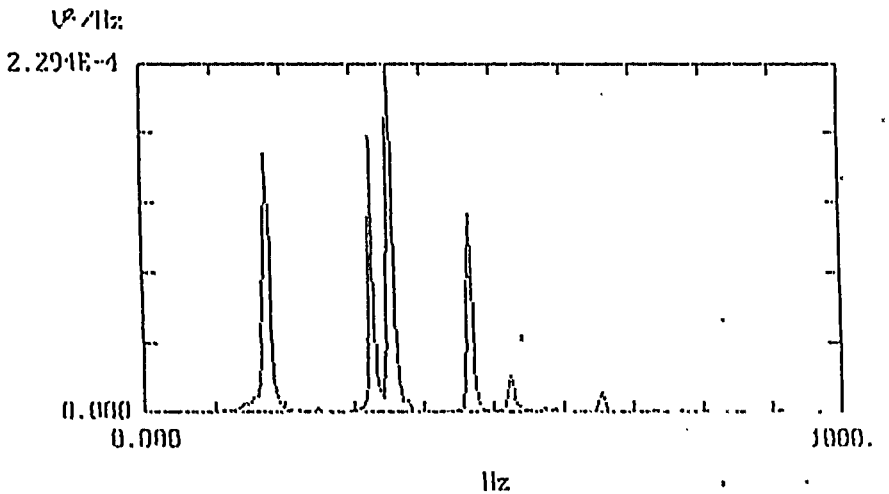

SG#C 1.5 amps

D:WOLFE\DATA\10419.DAT channel 3 :10AUG90 ACOUS TEST 146db (TOTAL)

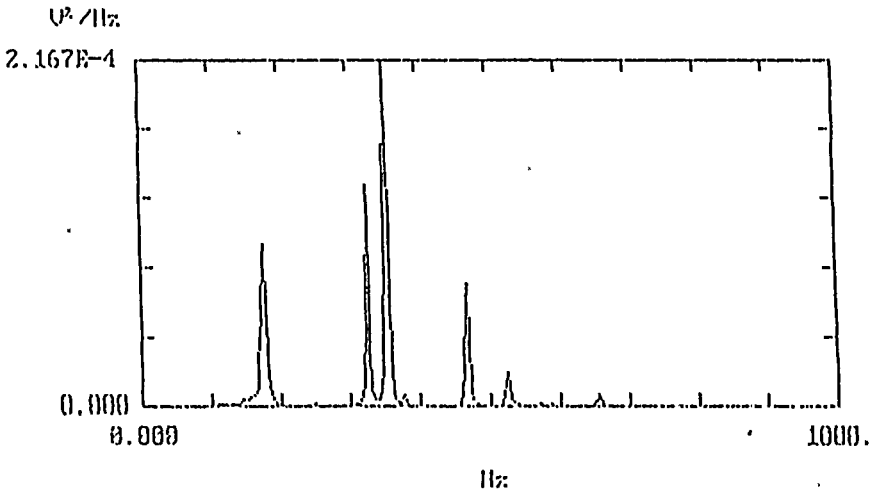

SG#7 1.7 amps

D:WOLFE\DATA\10415.DAT channel 3 :10AUG90 ACOUS TEST 146db (TOTAL)

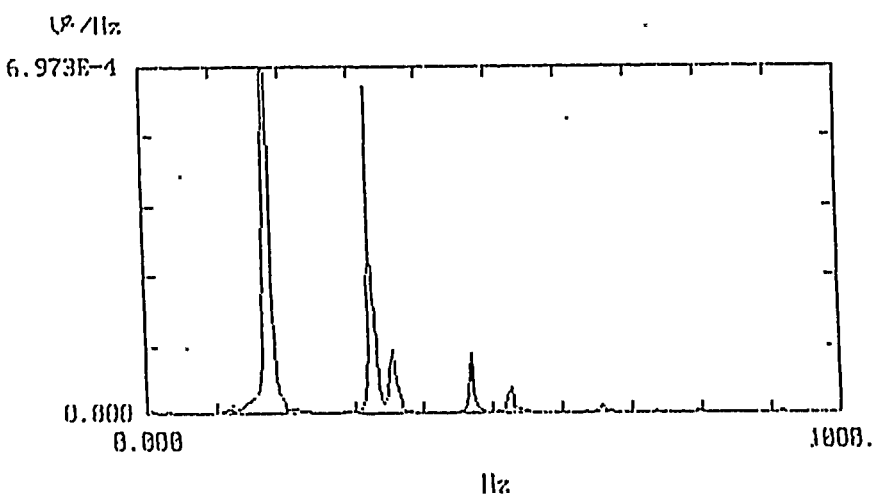

FIGURE 43: PSD STRAIN GUAUGE PAIRS 1 & 6 and 2 & 7 146 dB O/A